Zootaxa 5785 (1): 001–043
https://www.mapress.com/zt/

Article

ISSN 1175-5326 (print edition)
ZOOTAXA
ISSN 1175-5334 (online edition)

https://doi.org/10.11646/zootaxa.5785.1.1
http://zoobank.org/urn:lsid:zoobank.org:pub:C9DBE96C-912D-43FE-8D72-B6FD886AC3FF

Five new *Amphibolips* Reinhard, 1865 (Hymenoptera, Cynipidae) species from western and southern Mexico: expanding the diversity of oak gall wasps and revealing the largest oak apple gall in the Americas

DOHUGLAS ELISEO CASTILLEJOS-LEMUS[1,2*], KEN OYAMA[1,3], Y. MILES ZHANG[4], SUSANA VALENCIA-A[5] & JOSÉ LUIS NIEVES-ALDREY[6]

[1]*Escuela Nacional de Estudios Superiores Unidad Morelia, Universidad Nacional Autónoma de México (ENES-Morelia, UNAM). Antigua Carretera a Pátzcuaro 8701, Ex-Hacienda de San José de la Huerta, 58190, Morelia, Michoacán, México.*
[2]*Posgrado en Ciencias Biológicas, Unidad de Posgrado, Edificio D, 1° Piso, Circuito de Posgrados, Ciudad Universitaria, Coyoacán, C.P. 04510, CDMX, México.*
d.castillejos-lemus@enesmorelia.unam.mx; *https://orcid.org/0000-0002-0013-5242*
[3]*Laboratorio Nacional de Análisis y Síntesis Ecológica, ENES-Morelia, UNAM. Antigua Carretera a Pátzcuaro 8701, Ex-Hacienda de San José de la Huerta, 58190, Morelia, Michoacán, México.*
kenoyama@enesmorelia.unam.mx; *https://orcid.org/0000-0002-0367-1964*
[4]*Institute of Ecology and Evolution, Ashworth Laboratories, University of Edinburgh, Edinburgh, UK.*
yuanmeng.zhang@gmail.com; *https://orcid.org/0000-0003-4801-8624*
[5]*Herbario de la Facultad de Ciencias, Departamento de Biología Comparada, Universidad Nacional Autónoma de México, Ciudad de México, México.*
svalenciaa.unam@gmail.com; *https://orcid.org/0000-0003-4017-2387*
[6]*Museo Nacional de Ciencias Naturales (CSIC), Departamento de Biodiversidad y Biología Evolutiva, C/ José Gutiérrez Abascal 2, ES-28006 Madrid, Spain.*
jnievesaldrey@gmail.com; *https://orcid.org/0000-0002-4711-7455*
**Corresponding author*

Abstract

Five new species of oak gall wasps of the genus *Amphibolips* Reinhard, 1865 (Cynipidae, Cynipini) are described from Mexico. *Amphibolips megalokokka* Nieves-Aldrey & Castillejos-Lemus **sp. nov.** and *Amphibolips oyamai* Castillejos-Lemus & Nieves-Aldrey **sp. nov.** from the Trans-Mexican Volcanic Belt (TMVB) exhibit unique morphological characteristics within the genus, particularly in gall morphology. Three additional species, *Amphibolips zapoteco* Nieves-Aldrey & Castillejos-Lemus **sp. nov.**, *Amphibolips idiopteryx* Nieves-Aldrey & Castillejos-Lemus **sp. nov.** and *Amphibolips darioi* Castillejos-Lemus & Nieves-Aldrey **sp. nov.**, are described from Oaxaca State. These Oaxacan species show remarkable morphological similarity while providing important insights into the relationships among species within the Oaxacan clade. Based on a prior phylogenetic study using ultraconserved elements, we describe these five new species with supporting evidence from both morphology and molecular data. We also examined the great morphological variation in Trans-Mexican Volcanic Belt species, including both generations of one species, and discusses species richness, phylogenetic relationships, and taxonomic challenges within the genus.

Key words: Cynipini, *Lobatae*, Oaxaca, *Quercus*, taxonomy, Trans-Mexican Volcanic Belt

Introduction

The past decades have seen several taxonomic rearrangements within Cynipini (Hymenoptera: Cynipidae) across the American continent. This is evident in the description of new genera, taxonomic revisions, and the re-establishment of genera previously synonymized in recent reviews (Nicholls *et al*. 2018; Cuesta-Porta *et al*. 2020b; Nieves-Aldrey *et al*. 2021; Melika *et al*. 2021a, 2021b; Zhang *et al*. 2021). Traditional cynipid taxonomy has long faced difficulties in delineating genera due to morphological ambiguities. However, molecular techniques now provide clearer phylogenetic insights, leading to ongoing taxonomic revisions.

Accepted by S. van Noort: 19 Feb. 2026; published: 27 Mar. 2026

The Nearctic region, particularly Mexico, represents a biodiversity hotspot for oak gall wasps, with estimates suggesting over 700 species (Stone *et al*. 2002; Liu *et al*. 2007). This diversity is closely tied to the rich diversity of plants of the genus *Quercus* with more than 90 species in the United States and Canada, and 161 in Mexico (Valencia 2004; Liu & Ronquist 2006). In Mexico, the most recent Cynipini revision (Martínez-Romero *et al*. 2022) listed 205 species— a substantial increase from the 183 species recorded in the revision by Pujade-Villar & Ferrer-Suay (2015). Remarkably, just since Martínez-Romero *et al*. (2022), new descriptions have elevated this number to over 220 species (Cuesta-Porta *et al*. 2024; García-Martiñón *et al*. 2024; Castillejos-Lemus *et al*. 2025), with further increases expected as sampling efforts intensify and taxonomic studies progress.

To date, Cynipini species in Mexico have been exclusively associated with *Quercus* hosts (Liljeblad *et al*. 2008). A notable characteristic of Cynipini is the occurrence of alternating generations (asexual and sexual) in most species (Stone *et al*. 2002). However, few studies have investigated these alternating generation in Mexican species (Barrera-Ruíz *et al*. 2023). The impact of "closing" these life cycles (i.e., linking the two generations) on the current taxonomic nomenclature of Cynipini remains unclear, as this may reveal that numerous currently accepted species represent alternate-generations of the same taxon originally described separately (Cuesta-Porta *et al*. 2022; Nicholls *et al*. 2022; Sottile *et al*. 2022).

Amphibolips Reinhard, 1865 is a large genus of Cynipini found exclusively in the Americas. Currently, 62 species of *Amphibolips* are recognized, distributed across the Nearctic and Neotropical regions. Of these, 28 species occur in the United States and Canada, 30 in Mexico, two in Panama, one species is shared between Mexico and Panama, and another between Mexico and the United States (Kinsey 1937; Burks 1979; Melika & Abrahamson 2002; Medianero & Nieves-Aldrey 2010; Melika *et al*. 2011; Nieves-Aldrey *et al*. 2012; Pujade-Villar *et al*. 2018; Castillejos-Lemus *et al*. 2020, 2025; Cuesta-Porta *et al*. 2020, 2021, 2023, 2025; Nicholls *et al*. 2022). Notably, the genus *Amphibolips* is exclusively associated with the *Lobatae* section of the genus *Quercus*, which is also restricted to the American continents (Nieves-Aldrey *et al*. 2012).

Amphibolips is arguably one of the most studied genera of cynipid wasps in the Americas, subject to extensive taxonomic, functional, and genetic studies (Kariñho-Betancourt *et al*. 2019, 2020; Castillejos-Lemus *et al*. 2020, 2025; Cuesta-Porta *et al*. 2020, 2021, 2023, 2025; Nicholls *et al*. 2022). The morphological characteristics of adult wasps and their galls are remarkably consistent among closely related species. Galls induced by this genus typically develop on buds, stems, or leaves and, less commonly, on acorns. They are often globose or spindle-shaped and detachable, with spongy parenchyma surrounding a central larval cell (Beutenmüller 1909; Kinsey 1937; Melika & Abrahamson 2002).

Recent revisions and species descriptions have focused on morphological traits to distinguish two proposed species complexes within *Amphibolips*: the *nassa* and *niger* complexes (Cuesta-Porta *et al*. 2020, 2021, 2023). Marked morphological differences in adult wasps have led to hypotheses suggesting that the *niger* complex may represent a distinct but closely related genus or may constitute alternate generations within the *nassa* complex (Nieves-Aldrey *et al*. 2012; Castillejos-Lemus *et al*. 2020, 2025; Cuesta-Porta *et al*. 2020, 2021, 2023). The latest study on the *niger* complex, which included genetic evidence, did not yield conclusive support for either hypothesis (Cuesta-Porta *et al*. 2023).

Until 1937, only eleven *Amphibolips* species were known from Mexico (Bassett 1890; Beutenmüller 1911, 1917; Kinsey 1937). A significant increase in new species descriptions followed the work of Melika *et al*. (2011), who described two new species and proposed the *nassa* complex for species previously excluded from Kinsey's (1937) *niger* complex. Since 2011, twenty-one new *Amphibolips* species have been described in Mexico (Melika *et al*. 2011; Nieves-Aldrey *et al*. 2012; Pujade-Villar *et al*. 2018; Castillejos-Lemus *et al*. 2020, 2025; Cuesta-Porta *et al*. 2020, 2021, 2023. 2025), generating a debate regarding the validity and scope of the *nassa* complex (Melika *et al*. 2011; Nieves-Aldrey *et al*. 2012; Cuesta-Porta *et al*. 2020, 2023; Castillejos-Lemus *et al*. 2025).

Castillejos-Lemus *et al*. (2025) conducted a comprehensive phylogenetic analysis of *Amphibolips*, incorporating numerous described and undescribed species. According to recent taxonomic criteria (Cuesta-Porta *et al*. 2020), all wasps examined in Castillejos-Lemus *et al*. (2025) belong to the *Amphibolips nassa* complex. Notably, the 2025 study reaffirms *A. malinche* Nieves-Aldrey & Pascual, 2012 as a valid species in Mexico, a finding that diverges from the taxonomic proposal of Cuesta-Porta *et al*. (2020). Cuesta-Porta *et al*. (2020) introduced novel morphological characters to refine species delimitation within the *nassa* complex, with a focus on Mexican and Panamanian taxa. Notably, Cuesta-Porta *et al*. (2020) observed that some species distributed north of Mexico may occasionally exhibit morphological similarities to this newly defined complex. The disjunct distribution of certain *nassa* complex species, highlighted by Cuesta-Porta *et al*. (2020), suggests potential vicariant events or long-distance dispersal.

The phylogenetic study by Castillejos-Lemus *et al*. (2025) revealed four major evolutionary groups (clades) in *Amphibolips*, each with distinct physical traits and geographic ranges. Clade IV is distinctive because: (1) it contains almost exclusively Mexican species (except *A*. *castroviejoi* Medianero & Nieves-Aldrey, 2010 in Panama); (2) all species specialize on oaks from the *Erythromexicana* group of *Quercus* (Hipp *et al*. 2020); and (3) it comprises three regional subgroups - Oaxacan (southern Mexico), Sierra Madre Occidental (SMOc, western Mexico), and Trans-Mexican Volcanic Belt (TMVB, central Mexico). These subgroups showed such remarkable morphological similarity that reliable species differentiation remains problematic even for trained taxonomists.

The primary objective of this study is to formally describe and diagnose five new species within the genus *Amphibolips*, which were identified as undescribed lineages in the phylogeny of Castillejos-Lemus *et al*. (2025). Our work advances the alpha taxonomy of a biologically distinct and under-sampled group, providing the foundational data necessary for future ecological and evolutionary studies on gall wasps.

Material and methods

Study material

We sampled *Quercus* species of the *Lobatae* section in Jalisco, Michoacán, Mexico State, and Oaxaca in 2017–2018. The collected galls were stored in plastic containers with plastic or mesh lids, until the emergence of the wasps under laboratory conditions. The voucher specimens and their galls were deposited in the entomological collections of the Museo Nacional de Ciencias Naturales in Madrid, Spain, in the Colección Nacional de Insectos of the Instituto de Biología, Universidad Nacional Autónoma de México (UNAM), Mexico City, Mexico and in Escuela Nacional de Estudios Superiores Unidad Morelia, UNAM, Michoacán, Mexico. Dr Susana Valencia-Ávalos identified the host *Quercus* species, and voucher specimens were deposited in the Herbarium of the Facultad de Ciencias of the UNAM (FCME). Observations of habitats, geographic distribution and host affinities to *Quercus* species were mainly based on Valencia-Ávalos (2004) and other publications on *Quercus* species.

Molecular Analysis

All molecular data was generated for Castillejos-Lemus *et al*. (2025), with voucher specimens deposited in the Museo Nacional de Ciencias Naturales (Madrid, Spain), the Laboratorio de Ecología Genética y Molecular, Escuela Nacional de Estudios Superiores Unidad Morelia (Mexico), and the National Museum of Natural History (USA).

A modified version of the Castillejos-Lemus *et al*. (2025) phylogeny is presented for the 80% complete concatenated matrix under a maximum likelihood (ML) framework in IQ-TREE v2.2.6 (Minh *et al*. 2020). We performed 1000 ultrafast bootstraps (UFBoot; Hoang *et al*. 2018) and 1000 SH-like approximate likelihood ratio tests (SH-aLRT; Guindon *et al*. 2010), and nodes with UFBoot ≥ 95% and SH-aLRT ≥ 80% were considered well-supported. Resulting raw tree output was modified using R packages ggtree (Yu *et al*. 2017) and treeio (Wang *et al*. 2020) in R v4.5.1 (R Core Team, 2025).

Examination of types

We examined the type and paratype specimens of *Amphibolips oaxacae* Nieves-Aldrey & Pascual, 2012 and *A*. *nigrialatus* Nieves-Aldrey & Castillejos-Lemus, 2020 for comparison with the new species described from Oaxaca state. Additionally, we examined the type and paratype specimens of *A*. *nassa* Kinsey, 1937, *A*. *michoacaensis* Nieves-Aldrey & Maldonado, 2012, *A*. *tarasco* Nieves-Aldrey & Pascual, 2012, *A*. *nevadensis* Nieves-Aldrey & Pascual, 2012, *A*. *malinche*, and *A*. *jaliscensis* Nieves-Aldrey & Pascual, 2012 for comparison with the new species described from Jalisco and Michoacán states.

Specimen preparation

We generated the images used for the morphological descriptions with a FEI Quanta 200 (Oregon, US) scanning electron microscope (SEM) in Madrid (Spain) and with a JEOL JSM-IT300 (Tokyo, Japan) SEM in Morelia. For the SEM observations, we followed two strategies, depending on the number of individuals available for a given species. For the preservation of some unique specimens mounted in a conventional manner, we used a low vacuum technique without gold coating. When the number of specimens allowed it, we dissected some specimens in 99% alcohol and mounted in stubs to be coated with gold and observed with a high vacuum technique. We mounted the fore wings on slides in euparal and examined using Wild MZ8 and Olympus SZX10 stereomicroscopes. We acquired the images of the wings and adult habitus with a NIKON Coolpix 4500 digital camera attached to a Wild MZ8 light microscope, or an Olympus SC100 camera with the CELLSENS STANDARD software. We took measurements with a micrometric eyepiece calibrated to a Wild M5A stereomicroscope and an Olympus SZX10 stereomicroscope, photographed galls in their natural habitat using a Nikon D5300 camera, and images of the dissected galls were taken using a Huawei P30 mobile phone.

Morphological terms

We follow the terminology of morphological structures and abbreviations from Ronquist & Nordlander (1989), Nieves-Aldrey (2001) and Liljeblad *et al.* (2008). For wing venation, we followed Ronquist & Nordlander (1989) and for the terminology of the fore wing cells, we followed Weld (1964) and Richards & Davies (1977). For sculpture terminology, we followed Harris (1979). The measurements of the structures were made according to Nieves-Aldrey (2001). The abbreviations used include **F1**–**F13** for the antennal flagellomeres, **POL** (post-ocellar distance) for the distance between the inner margins of the posterior ocelli, **OOL** (ocellar-ocular distance) for the distance from the outer margin of a posterior ocellus to the inner margin of a compound eye and **DOL** (diameter of a lateral ocellus).

Institutional abbreviations

MNCN Museo Nacional de Ciencias Naturales, Madrid, Spain
ENES-Morelia Escuela Nacional de Estudios Superiores, Unidad Morelia, Mexico
CNIN Colección Nacional de Insectos, Instituto de Biología, UNAM, Mexico
USNM National Museum of Natural History, Smithsonian, Washington DC, USA.

Results

Diagnosis and comments of clade IV of *Amphibolips*

Females can be broadly categorized into two wing-pattern types: (1) species characterized by a dark band running along the anterior fore wing margin, extending from the base to the apex; and (2) species displaying generalized dark coloration over most of the wing, interspersed with hyaline bands (which can sometimes be quite broad). Some species exhibit intermediate or variable patterns that appear to blend these two types. Males of clade IV (Fig. 1) typically exhibit entirely smoky wings, although these sometimes resemble the considerably darker manifestations of the female wing patterns. This clade is restricted to the region from Mexico to Panama and is closely associated with oak species of the *Erythromexicana* group (sensu Hipp *et al*. 2020).

Within clade IV, three well-defined lineages were identified (Castillejos-Lemus *et al*. 2025): Oaxaca, SMOc, and TMVB + South SMOc. The SMOc lineage exclusively exhibits the generalized dark wing pattern with hyaline bands. In contrast, the TMVB + South SMOc lineage is characterized by a predominantly hyaline posterior wing with coloration restricted to the anterior band (Figs 5C, 9B, 18E, G, H). The Oaxaca lineage can be subdivided based on the same wing-pattern criteria. One group within it shows the anterior dark band; however, when a translucent region is present distally, it does not extend beyond a single wing cell (typically the third cubital cell).

Galls within clade IV develop from buds and tend toward two principal morphological types: semi-spherical galls with spongy parenchyma or spindle-shaped galls with firm-textured parenchyma. An intermediate form, potentially represented by galls such as those of *A. magnigalla* Nieves-Aldrey & Castillejos-Lemus, 2020, may combine spongy parenchymal tissue with a thicker epidermis. Notably, some spherical galls possess thin, radiating filaments that are often obscured by the spongy tissue.

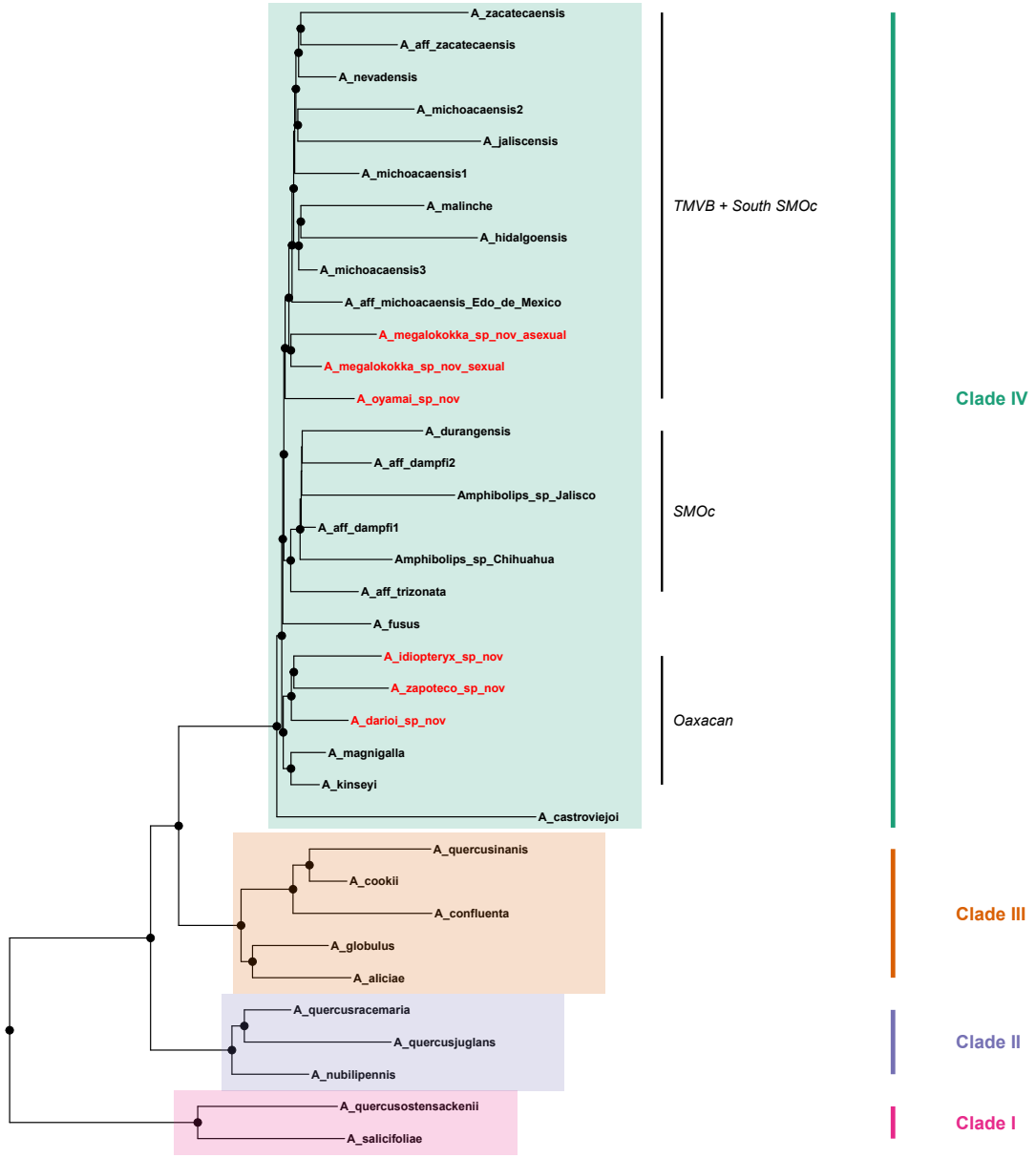

FIGURE 1. Phylogeny of *Amphibolips*. IQ-TREE tree result of Maximum Likelihood analysis using the SWSC-EN partitioning scheme with the 80% matrix. Four clades proposed here are highlighted in different colors and numbered according to the text. Nodes with black dots indicate support values of UFBoot > 95 and SH-aLRT > 80.

Amphibolips megalokokka Nieves-Aldrey & Castillejos-Lemus sp. nov.

urn:lsid:zoobank.org:act:9C6240B2-4CB5-4DBC-AF4F-D25BE72A1978
Figs 2–7

Type material.

Holotype.

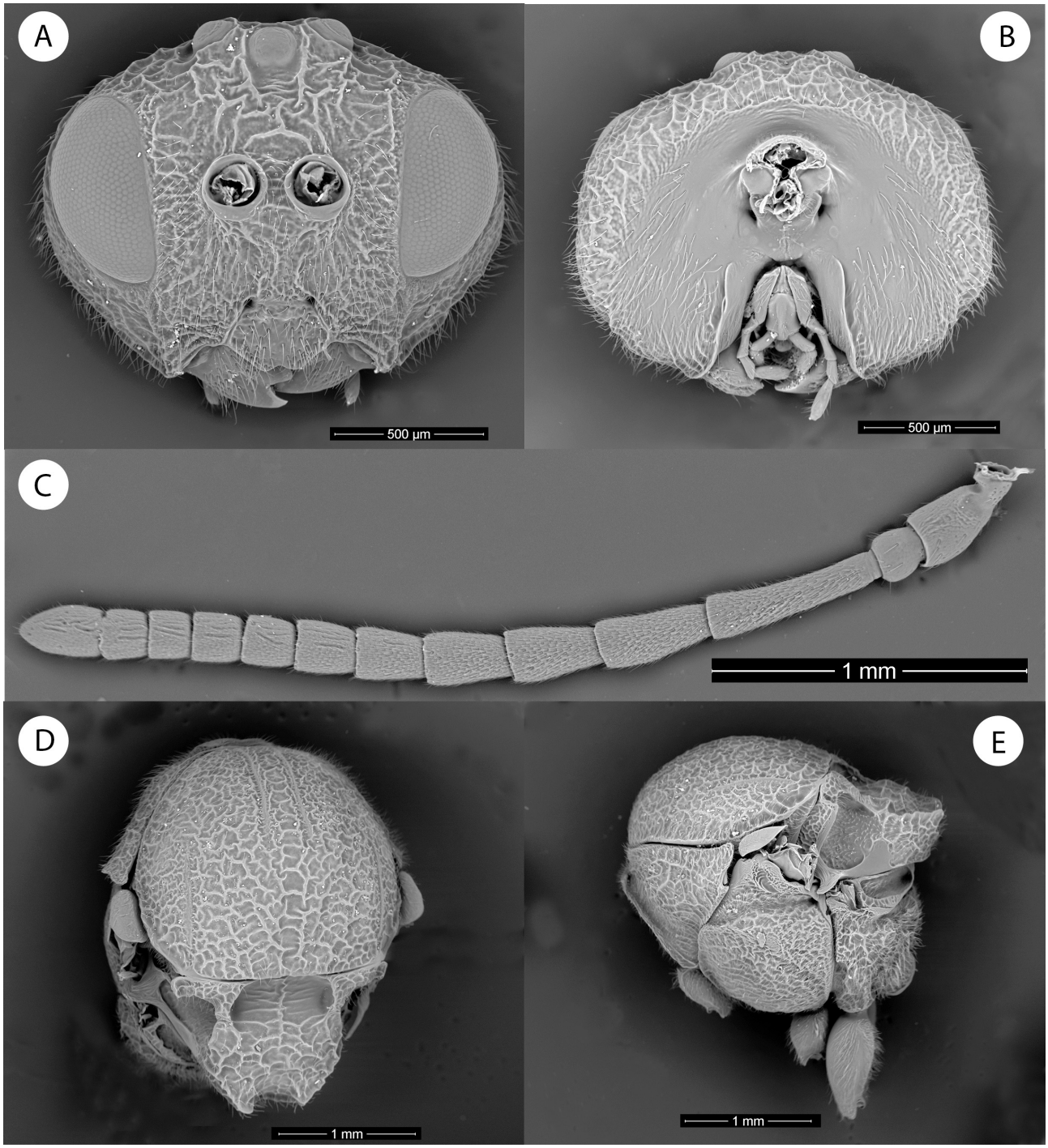

FIGURE 2. *Amphibolips megalokokka* sp. nov., sexual female **A** head, anterior view **B** head, posterior view **C** antenna **D** mesosoma, lateral view **E** mesosoma, dorsal view.

MEXICO • female; Jalisco, Talpa de Allende, El Cuale; 20°21.492'N, 105°00.99'W; 2484 m a.s.l.; 10 Apr. 2018; D. Castillejos-Lemus leg.; ex gall on *Quercus scytophylla* (*Quercus* sect. *Lobatae*), insect emerged Apr–May 2018; mounted on a card in MNCN.

Paratypes.

MEXICO • 6f 3m; same data as holotype; mounted on cards in MNCN • 2f 1m; same data as holotype; GenBank: SRX25798179 (individual code Amphibolips_sp_nov1_Jalisco244); mounted on stubs for SEM observation in MNCN • 1f 3m; same data as holotype; preserved in alcohol at MNCN • 10f; same data as holotype; mounted on cards in ENES-Morelia and CNIN • 7f; same data as holotype; preserved in alcohol at ENES-Morelia • 1m; same

data as holotype; extracted dead from a gall on 22 Nov. 2024; stored in a dry tube at ENES-Morelia • 1f; same collection location; 20.37786°N, 105.10567°W; 2048 m a.s.l.; 14 Nov. 2017; D. Castillejos-Lemus leg.; ex gall on *Quercus cualensis* (*Quercus* sect. *Lobatae*), insect emerged 16 Feb. 2018; GenBank: SRX25798246 (individual code Amphibolips_sp_nov1_JaliscoNM); mounted on a card at ENES-Morelia.

Additional material (only galls).

MEXICO • 48 galls; same data as holotype; 3 dissected and 45 complete; in ENES-Morelia and CNIN • 6 galls; same data as the paratype from *Quercus cualensis*; 2 dissected and 4 complete; in ENES-Morelia and CNIN.

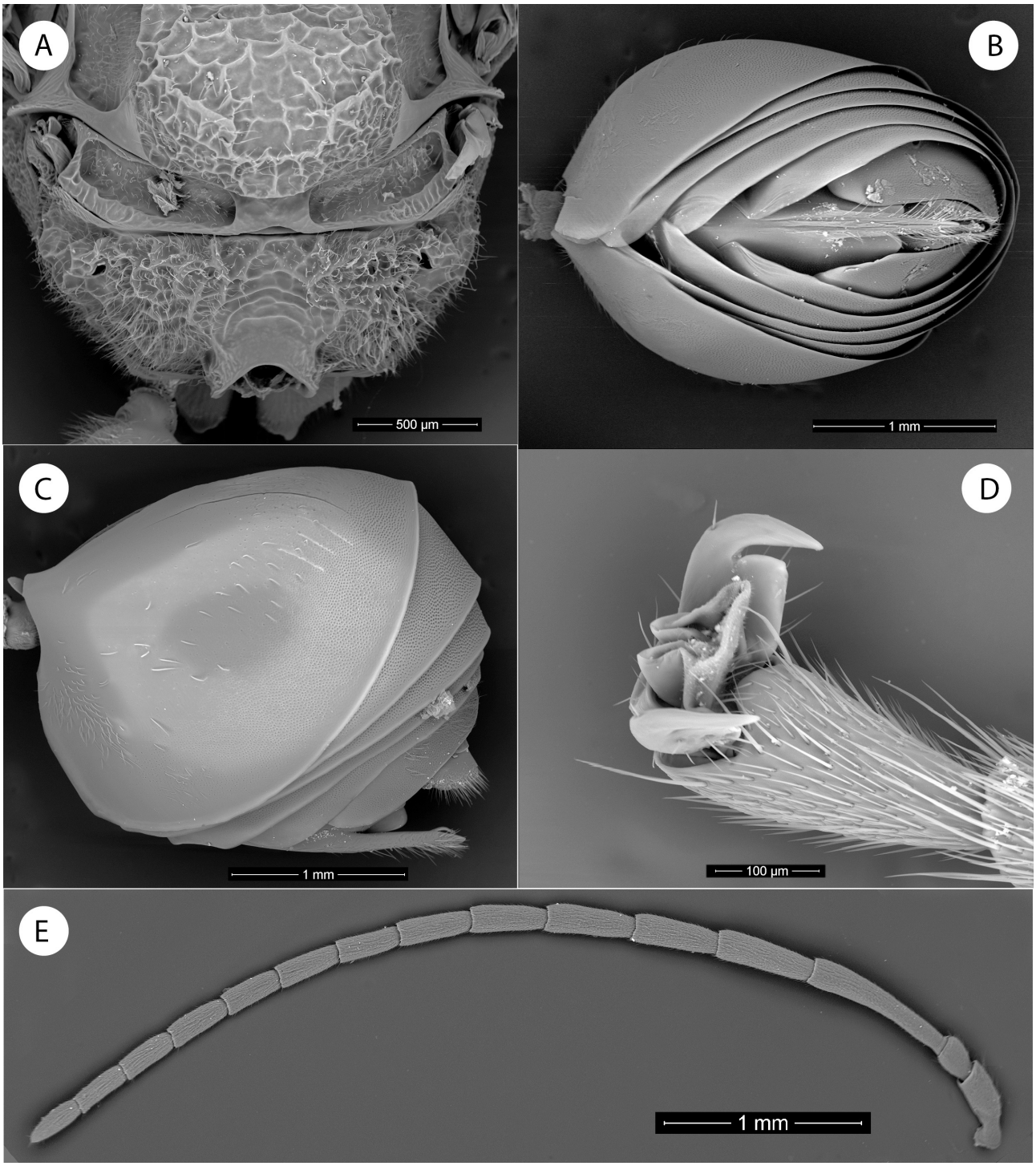

FIGURE 3. *Amphibolips megalokokka* sp. nov., sexual generation **A** female mesoscutellum and propodeum **B** female metasoma, ventral view **C** female metasoma, lateral view **D** female metatarsal claw **E** male antenna.

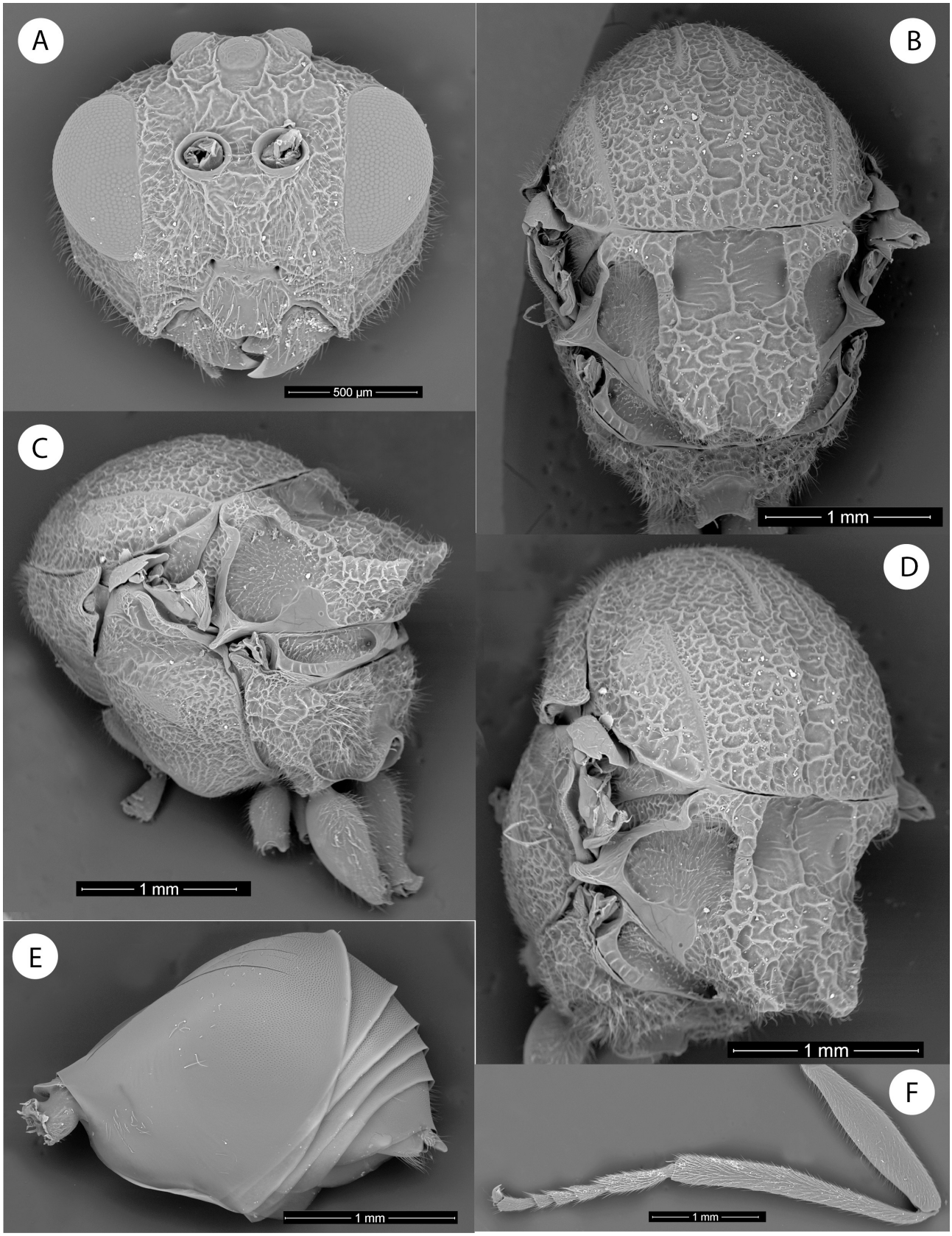

FIGURE 4. *Amphibolips megalokokka* sp. nov., sexual male **A** head, anterior view **B** mesosoma, dorsal view **C** mesosoma, lateral view **D** mesosoma, dorsolateral view **E** metasoma, lateral view **F** leg.

Etymology.

The species name *megalokokka* derives from the Greek *megalos* (μεγάλος), meaning "large", and *kokkos* (κόκκος), meaning "grain" or "berry". The name refers to the large, spherical gall induced by the species. The feminine ending *–kokka* agrees with the genus *Amphibolips*, following zoological nomenclature rules.

Diagnosis.

Amphibolips megalokokka belongs to clade IV, characterized by a less infuscated region in the distal part of the radial cell (Fig. 5C), which also includes *A. jaliscensis*, *A. malinche*, and *A. hidalgoensis* Pujade-Villar & Melika, 2011. Furthermore, based on their distribution and morphology, *Amphibolips nassa*, *A. rulli* Pujade-Villar & Cuesta-Porta, 2020, *A. chilito* Pujade-Villar & Cuesta-Porta, 2025, and *A. tarasco* are also hypothesized to belong to this clade. *Amphibolips megalokokka* can be readily distinguished from *A. rulli* by the punctate sculpture that *A. rulli* exhibits (projecting anteriorly onto the dorsum of the second metasomal tergum; Fig. 19D), which is absent in all other species. In *A. megalokokka* the coriaceous-alutaceous sculpture (Fig. 3C) extends posteriorly across the second metasomal tergum, resulting in a reduction of the micropunctate band medially (inverse to the pattern observed in *A. rulli*). It is distinguished from all these species by the pigmentation of the costal cell, which is more intense and extensive in *A. megalokokka* and barely perceptible (or absent) in all other species of this clade (this even applies to the asexual generation). *A. megalokokka* also exhibits pigmentation on the posterior margin of the anal cell, located below the basal cell with a median location, which is scarcely visible in the other species of the clade. The sexual generation galls of *A. megalokokka* (Fig. 5E, F) are further distinguished from those of *A. hidalgoensis*, *A. malinche*, *A. zacatecaensis* Melika & Pujade-Villar, 2011, *A. michoacaensis*, *A. tarasco*, *A. chilito* and *A. oyamai* by their combination of dimensions, reddish coloration, completely round shape, and external texture. Disregarding dimensions, the most morphologically similar galls are those of *A. nevadensis* and *A. jaliscensis*.

Description (sexual generation).

Body length: 5.4 mm average (n = 10; 4.4 mm– 6.3 mm) for females.

Female (Fig. 5A)**:** Body almost black, particularly intense on the thorax, head, and most of the antenna. Frontal and distal parts of the antennal scape and pedicel usually chestnut. Last flagellomeres chestnut ventrally and black dorsally. Mandibles, and occasionally the region surrounding the mandibles, chestnut. Mesosoma usually black with the posterior region of the propodeum immediately posterior to the nucha chestnut. Some specimens may have a general posterior chestnut coloration instead of black, exhibit chestnut tegulae or operculum of the mesothoracic spiracle, or a combination of these characteristics. Tarsi typically range from light brown to dark brown from anterior to posterior. Fore and middle tibiae chestnut; posterior tibiae black. Some specimens exhibit chestnut coloration on all legs, but the intensity from light to dark is general, regardless of whether the coloration is never completely black. Metasoma usually black dorsally and chestnut ventrally. First metasomal tergum and the immediate anterior region of the second metasomal tergum adjacent to the first metasomal tergum chestnut. Posterior margins of the metasomal terga, posterior to the micropunctate bands, chestnut. Hypopygium and areas near the hypopygium and ventral spine chestnut, lighter on the ventral spine. Some specimens may have chestnut coloration throughout the metasoma, extending the anterior region of the metasoma (adjacent to the second metasomal tergum) to the smooth sides of the same metasomal tergum, to the ventral part of the metasoma, or a combination of these variations. Fore wing (Fig. 5C) with a dark infuscate band extending on the anterior margin along the basal cell, first cubital cell, radial cell, costal cell, and anterior margin, and joining the radial cell at the third cubital cell. The entire discoidal cell is hyaline. The costal cell has a hyaline area (or less intense pigmentation) at the junction of vein Rs with vein R+Sc, which can extend in some cases to the anterior margin of the wing. The anal cell is usually hyaline but exhibits a patch with greater pigmentation on the posterior margin of the wing at the mid-position relative to vein M+Cu1. Veins R+Sc, Rs, M, and the first half of R1 are black. The rest are chestnut or brown. Veins M (at the margin of the third cubital cell) and Cu1 are light brown and are usually the lightest compared to the other wing veins. The wing pigmentation shows several variation patterns: (1) a less pigmented area in the posterior half of the radial cell (including the posterior half of vein Rs bordering the cell); (2) complete division of the typical clade band toward the third cubital cell; (3) extension across both margins of vein Rs bordering the radial cell; or (4) nearly imperceptible depigmentation, appearing only as faint discoloration on vein Rs's posterior half (visible as vein color loss) and a small adjacent area in the third cubital cell. These variations may occur combined and, rarely, differ between wings of the same individual. Additionally, vein Rs+M shows about one-third (sometimes less) of its length depigmented at its junction with vein M.

Head: in dorsal view, 2.4 × wider than long (range 2.15–2.6). POL 1.2 × OOL (range 0.9–1.4) and 1.9 × DOL (range 1.5–2.3). Head, in anterior view (Fig. 2A), 1.25 × wider than high, gena slightly broadened behind the eye. Vertex, frons, lower face, and gena with strong reticulate-rugose sculpture. Irradiating carinae from the clypeus absent. Head moderately pubescent, with pubescence sparser on the vertex and frons. Clypeus hexagonal, ventral margin strongly projecting over mandibles and sinuate on the anterior margin. Anterior tentorial pits clearly visible; epistomal sulcus and clypeo-pleurostomal lines weakly indicated. Malar space 0.45 × the height of the compound eye. Toruli situated at mid-height of the compound eye. Transfacial line 1.35 × the height of an eye. Distance between antennal rim and compound eye shorter than the width of the torulus including the rim. Ocellar plate slightly raised.

Head: in posterior view (Fig. 2B), moderately pubescent, with occiput coarsely rugose; dorsally the sculpture is slightly transversely ribbed. Two small carinae present, arising from the dorsal part of the occipital foramen, directed ventrally but not extending past the posterior tentorial pits. Posterior tentorial pits rounded. Gular sulci barely visible, united, meeting at the hypostoma. Posterodorsal margin of the oral foramen not emarginate medially. Hypostomal ridges well separated.

Mouthparts: Mandibles strong, exposed, with dense setae at the base. Cardo of maxilla not visible; maxillary stipes 3.7 × as long as wide. Maxillary palp with five segments. Labial palp with three segments. Apical peg of the last maxillary segment present.

Antenna (Fig. 2C)**:** of moderate length, 0.5 × the body length, with 13 antennomeres. Flagellomeres F10 and F11 partially divided. Flagellum not broadening towards apex, bearing short and erect setae. Pedicel short, small, as broad as long, 0.4 × the length of the scape. F1 1.6 × as long as F2. F7–F10 appear as long as wide. F11 1.6 × as long as wide, 1.7 × as long as F10. Placodeal sensilla present on F3–F11, arranged in dense rows from F4 onwards, located only on the ventral half of each flagellomere.

Mesosoma: in lateral view (Fig. 2E), 1.15 × as long as high. Pronotum pubescent; lateral surface of pronotum with strong, irregular, reticulate-rugose sculpture. Pronotum medially short, but slightly larger than in other species; median pronotal length 0.3 × that of lateral pronotal length. Pronotal plate slightly distinct dorsally. The central region of the pronotum is smooth and shiny, quite conspicuous and broad compared to the rest of the pronotum, which exhibits rugosities and pubescence.

Mesonotum: Mesoscutum (Fig. 2D) pubescent primarily on the anterior portion, but with setae very short and thin, thus only conspicuous in the anterior region adjacent to the pronotum. Sculpture reticulate-rugose, more noticeable posteriorly where the reticulations are larger and deeper; interspaces smooth and shining, interrupted only by setae on the anterior portion or by the reduced size of the reticulations. Notauli not discernible. Longitudinal median impression barely perceptible, only next to transscutal fissure. Anteroadmedian signa quite visible, extending posteriorly to near mid-length of mesoscutum. Parapsidal signa obscured by sculpture but discernible to mid-length of the mesoscutum. Transscutal fissure narrow, nearly straight, slightly sinuate in some specimens. Mesoscutellum slightly wider than long (ratio 0.9), approximately 0.6 × the length of mesoscutum. Strongly coarsely rugose, slightly pubescent, with a broad median longitudinal impression that makes the mesoscutellum emarginate posteriorly (Figs 2D, 3A); median longitudinal impression usually extends anteriorly to scutellar foveae, but occasionally the sculpture between margins and foveae interrupts in the center of mesoscutellum, giving a more elevated appearance. Scutellar foveae (Fig. 2D) 0.4 × the length of mesoscutellum, relatively square and usually deep, without pubescence, separated by a carina on the posterior half. With well-separated transverse rugae of variable length in each fovea and smooth interspaces. Axillula large, pubescent, but with setae small and very sparse, revealing the shiny and almost smooth background, not very deep and with posterior margin scarcely defined. In lateral view (Fig. 2E), the posterodorsal extension of the body of the subaxillular strip reaches one half of mesoscutellar height. Mesopleuron reticulate-rugose, pubescent, with rugae not as strong as in mesoscutum (Fig. 2E). Mesopleural triangle is shinier than the rest of mesopleuron, especially compared to the immediate area of mesopleuron that borders it, which is an opaque black color. Posterior groove in mesopleural triangle present below the tegula; smooth, resembling the deepest region of mesopleural triangle that borders the rest of mesopleuron, quite deep and delimited at its edges by rugae that resemble carinae.

Metanotum (Fig. 3A)**:** Metapectal-propodeal complex. Metapleural sulcus reaching the posterior margin of the mesopectus at approximately mid-height of the metapectal-propodeal complex. Metascutellum rugose and shiny. Metanotal trough pubescent. Propodeal area with irregular rugae. With pubescence, primarily on the sides; lateral propodeal carinae indistinct due to the rugae, but the reduced pubescence allows this area to appear shinier.

Legs: Densely pubescent, particularly on the tibiae and tarsi; femora and tibiae robust. Metatibia 1.7 × as long as the metatarsus; apical margin of metatarsomeres 1–4 with long, strong, erect setae (Fig. 3D). Metatarsal claws featuring prominent triangular basal lobes or teeth (Fig. 3D).

Fore wing (Fig. 5C)**:** slightly longer than the body. Radial cell 3.6 × longer than wide; open along the anterior margin. Areolet present. Veins M and Cu1 nearly straight, not reaching the wing margin. Rs+M complete, reaching the basalis at half its length, but with one-third (rarely less) unpigmented at its junction with vein M. First abscissa of radius (2r) curved, not projecting towards the radial cell. Vein Cu1 not branched into two veins. Apical margin with a very short or obsolete hair fringe. A slight fading present in most specimens at the end of radial cell, which in darker specimens appears only faintly on vein R1 and in a small area near the radial cell on the third cubital cell. The most densely pigmented regions are the basal cell and the first half of the radial cell, although in some specimens the pigmentation may be so intense that these regions are barely distinguishable from the rest of the pigmented band.

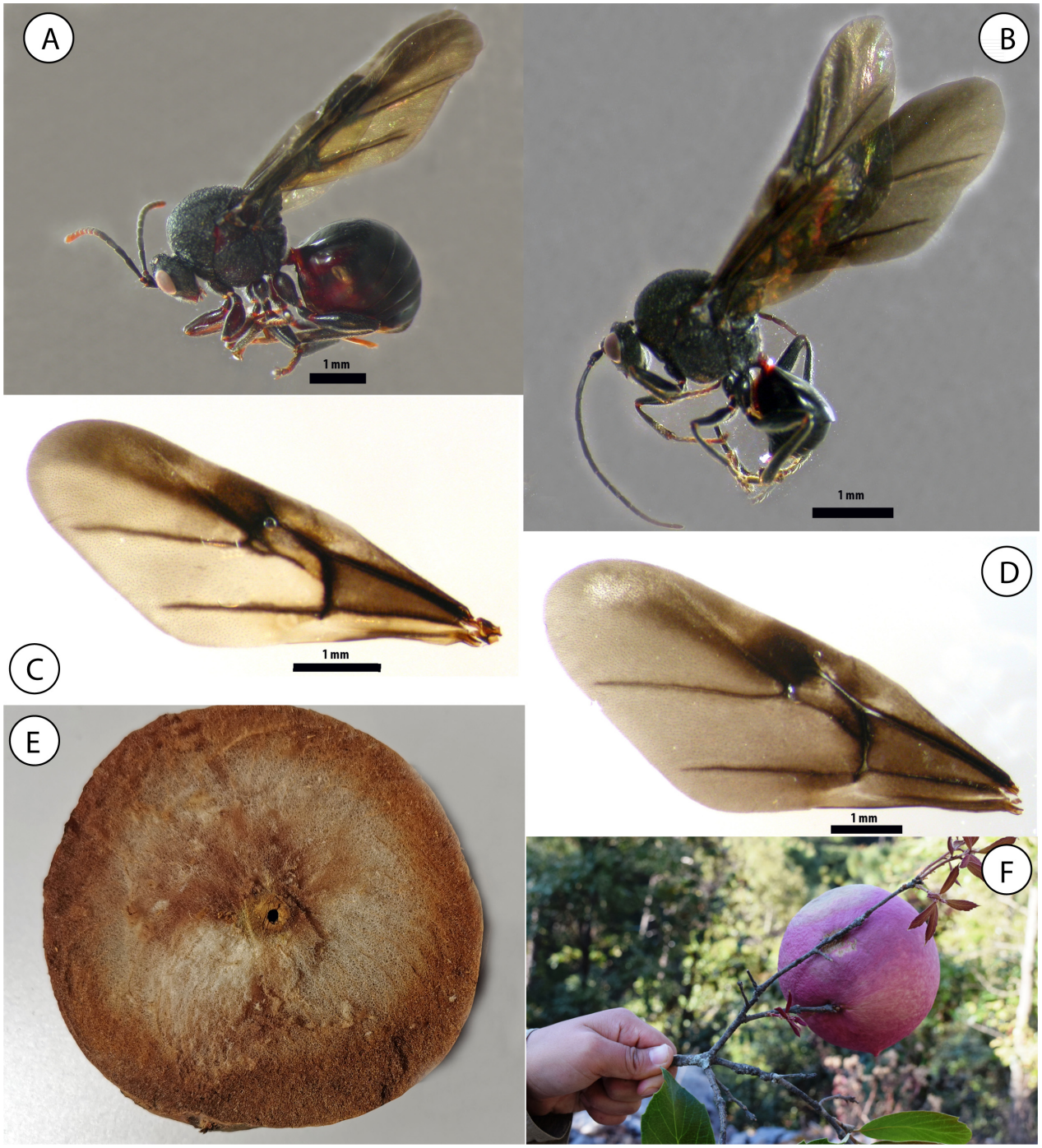

FIGURE 5. *Amphibolips megalokokka* sp. nov., sexual generation **A** female habitus **B** male habitus **C** female fore wing **D** male fore wing **E** section of a gall **F** gall.

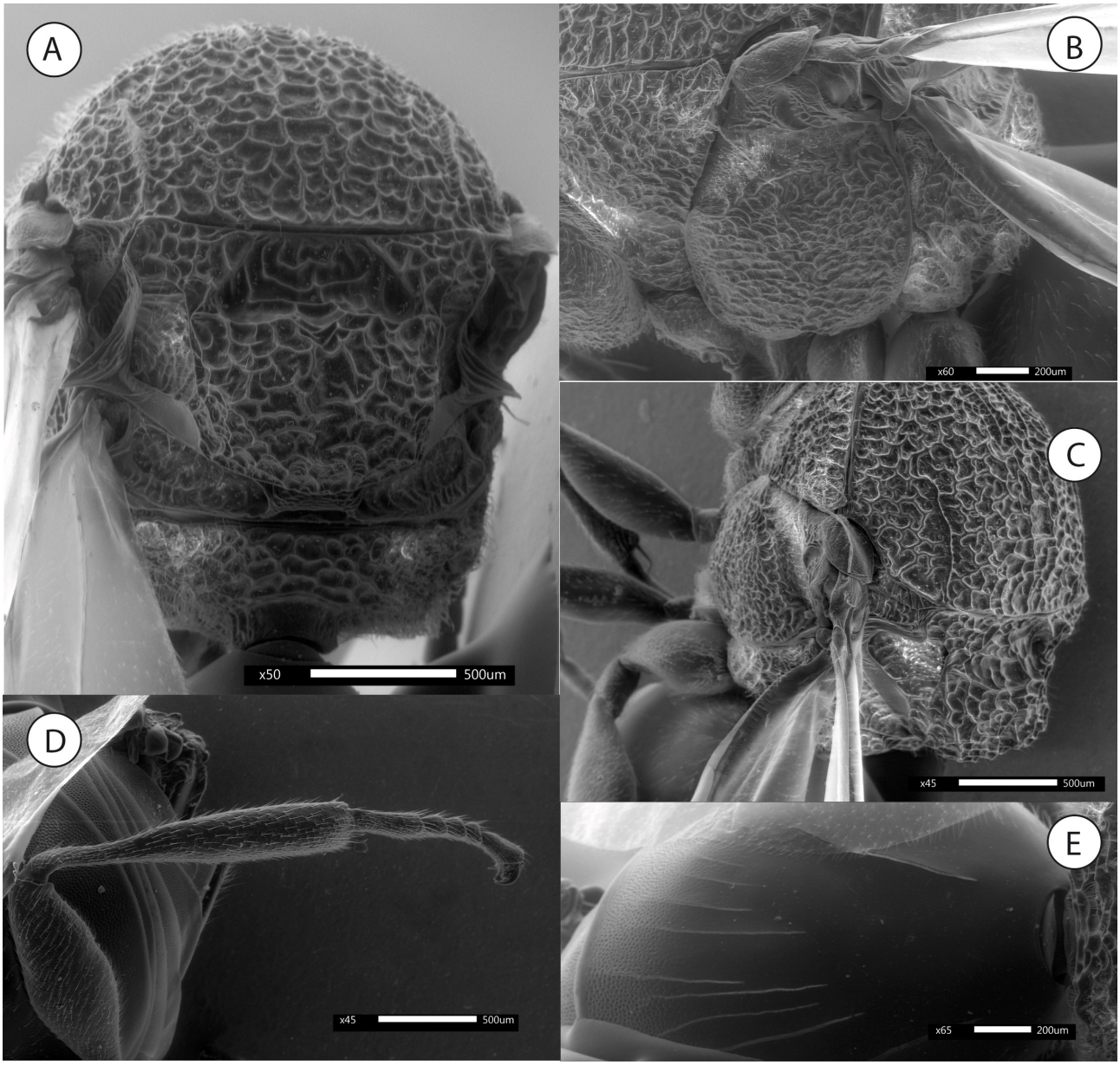

FIGURE 6. *Amphibolips megalokokka* sp. nov., asexual generation **A** mesoscutellum and propodeum **B** mesopleuron **C** mesosoma, dorsolateral view **D** leg **E** metasoma, dorsal view.

Metasoma (Figs 3B, C)**:** in dorsal view 1.5 × as long as wide, in lateral view 1.3 × as long as high. Second metasomal tergum covering approximately 0.6 × the length of the metasoma; anterior half smooth and shining, posterior third with a band of micropunctures clearly visible. In the second metasomal tergum, anterior to the area of micropunctures, there is a region with coriaceous-alutaceous sculpture, almost exclusively on the dorsal part, following the anterior smooth area. It exhibits a pattern where the band of micropunctures is narrower in the center (somewhat inverse to the pattern of *A. rulli*), with an extension of the coriaceous-alutaceous sculpture towards the band of micropunctures. The punctate sculpture extends onto subsequent terga. Ventral area of the second metasomal tergum moderately pubescent. Projecting part of the hypopygial spine long (Fig. 3B); 7.2 × as long as high in lateral view; ventrally tapering in width towards the apex, laterally with long setae that can reach the width of the ventral spine, not forming an apical patch.

Male: 5.1 mm (n = 1). Differs from the female as follows: Metasoma (Fig. 4E) smaller than the thorax (contrary in females). Antennae, legs, and wings longer relative to the body (Fig. 5B). Antennae with 15 antennomeres (Fig. 3E); F1 slightly modified, flattened on the ventral side, with elongate placodeal sensillae visible in all flagellomeres.

Clypeus shinier and smoother (Fig. 4A). Mesoscutellum more widely and deeply emarginated on the posterior margin (Fig. 4B–D), with the median longitudinal impression deeper and well-defined. Posterodorsal extension of the body of the subaxillular strip broader (Fig. 4C). Lateral propodeal carinae distinct in the anterior part. Metasoma with less ventral pubescence and coriaceous-alutaceous sculpture slightly visible (Fig. 4E). Metatibia 1.5 × as long as the metatarsus (Fig. 4F). Fore wings more heavily infuscate across their entire surface, but the darker anterior band and unpigmented regions remain visible, retaining the same pattern as in the female (Fig. 5D).

Asexual generation female. 4.6 mm (n = 1).

The paratype (1f) collected from galls on *Quercus cualensis* in November 2017 corresponds to a completely different date compared to all wasps obtained from the type locality. According to Castillejos-Lemus *et al*. (2025), species delimitation analyses confirm that this wasp and those from the type locality form a single monophyletic lineage, supporting their status as the same species (Fig. 1).

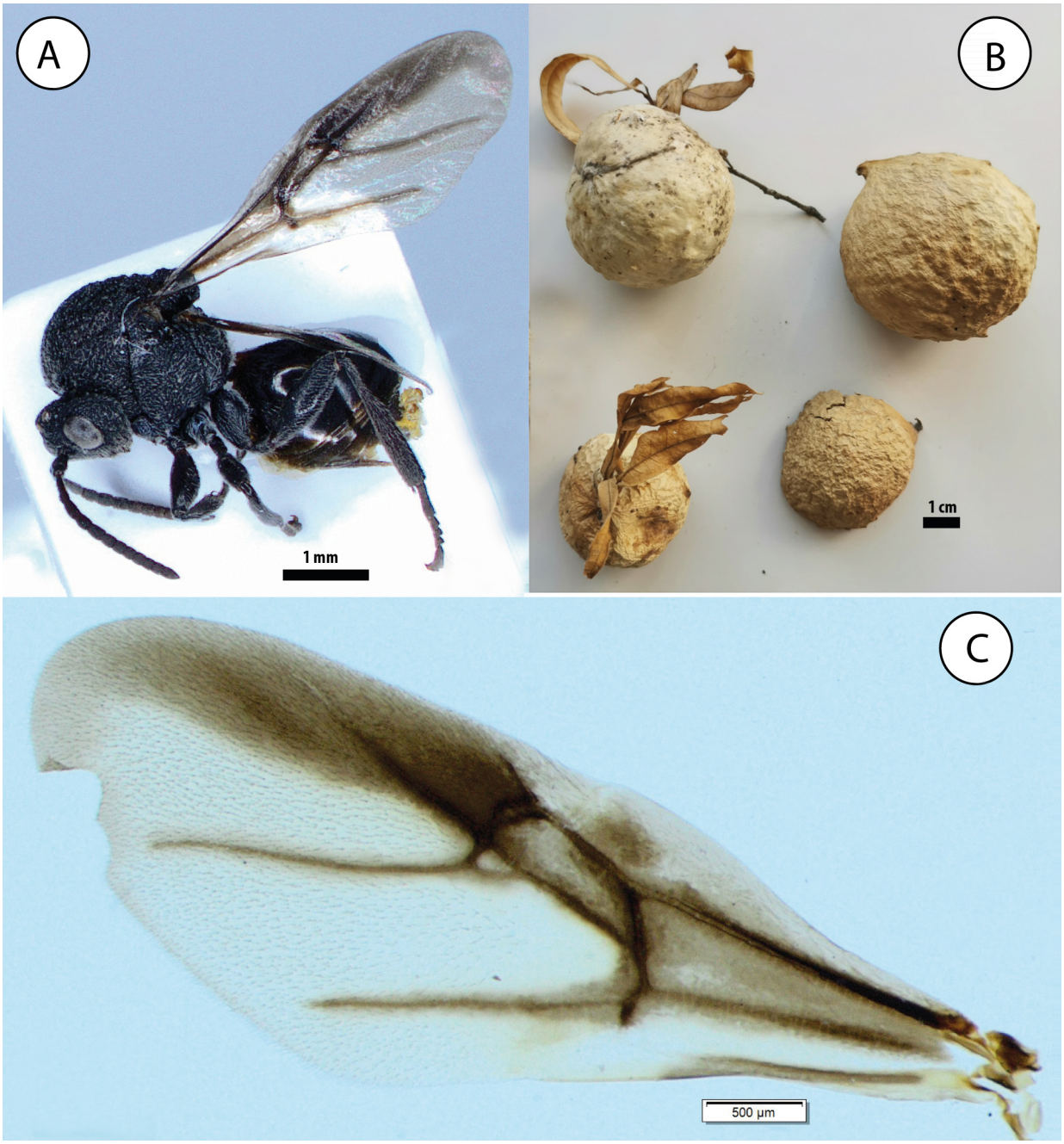

FIGURE 7. *Amphibolips megalokokka* sp. nov., asexual generation **A** habitus **B** galls **C** fore wing.

Differs from the sexual generation female as follows: Smaller in size compared to those of the sexual generation (Fig. 7A), measuring 4.6 mm, comparable to smallest females of the sexual generation (uncommon). Posterior groove of the mesopleural triangle (Fig. 6B, C), shallower. The notch delimiting mesopleural triangle, less pronounced (Fig. 6B, C). Median longitudinal impression of the mesoscutellum (Fig. 6A), narrow. No clear division between foveae. Posterior emarginations of mesoscutellum are almost imperceptible. Axilla, less shiny. Lateral propodeal carinae indiscernible (Fig. 6A). Metatibia exhibits distinct morphology (Fig. 6D): in sexual females, there is a gradual increase in width towards the distal part, whereas in asexual generation, this increase in width occurs at the end of the first third and is more pronounced. Radial cell (Fig. 7C), 3 × as long as wide. Coriaceous-alutaceous sculpture is almost absent on the dorsal part of the metasoma, similar to that observed in the male (Fig. 6E).

Gall (Figs 5E, F, 7B)**:** Two morphologies exist, corresponding to the two generations described for this species. The gall of the sexual generation (Fig. 5E, F) exhibits intermediate characteristics between those typical of the clade (TMVB + south SMOc; Castillejos-Lemus *et al*. 2025) and the galls of *A*. *oyamai*. This is the largest gall recorded for a single Cynipini wasp in the American continent, reaching slightly over 11 cm in diameter in the most extreme cases. This size is comparable to that of *A*. *magnigalla*, but being spherical rather than spindle-shaped, it results in a much larger volume, rivalling tuberous galls of the genus *Andricus* Hartig, 1840 in Mexico (multilocular). They are regularly spherical with a spongy inner consistency. The surface is smooth and soft to the touch. They are monothalamic. When fresh, they exhibit a reddish coloration. Similar to the galls of *A*. *oyamai*, when fresh, they can be easily torn by touch. As is typical for galls of this clade, the galls of this species turn light brown when dry, but those of *A*. *megalokokka* retain some of the reddish coloration. The galls of this species become slightly more resistant to touch when dry, as in *A*. *oyamai*. The epidermis is thin and firmly attached to the internal spongy tissue when fresh. Internally, the spongy tissue occupies the entire space between the epidermis and the larval chamber. The average longitudinal diameter is 10.2 cm, and the average transversal diameter is 7.5 cm (longitudinal diameter ranging from 41 to 112 mm and transversal diameter from 42 to 114 mm; n = 43). The galls of the asexual generation are considerably smaller (Fig. 7B). The average longitudinal diameter is 4.5 cm, and the average transversal diameter is 4.2 cm (longitudinal diameter ranging from 36 to 58 mm and transversal diameter from 35 to 47 mm; n = 6). This gall is similar to those described for other species of the same clade (TMVB + south SMOc; Castillejos-Lemus *et al*. 2025). Compared to the galls of the sexual generation, it is less smooth on the surface, with some scattered irregularities, and has a firmer consistency when fresh.

Distribution.

Amphibolips megalokokka was found in the Ejido El Cuale, in the municipality of Talpa de Allende, in Jalisco state, at elevations above 2000 meters above sea level (m a.s.l.). The approximate linear distance between the two sites is 9.6 km. Both locations are situated on the leeward side of the region, with an elevation difference of approximately 400 m a.s.l.

Biology.

Both generations are known. The galls of the sexual generation develop on *Quercus scytophylla*, while those of the asexual generation develop on *Q*. *cualensis*. In both cases, they occur above 2,000 m a.s.l. The galls of the sexual generation were collected in April, and the insects emerged in April and May. The galls of the asexual generation were collected in November, and the insects emerged in February of the following year. Smaller galls typically do not yield adult *Amphibolips* due to parasitoid attacks or the presence of inquilines. As a result, the average measurements of the galls from the sexual generation are influenced by these factors.

Remarks.

This wasp is assigned to the TMVB + south SMOc clade (as defined in Castillejos-Lemus *et al*. 2025).

Amphibolips oyamai Castillejos-Lemus & Nieves-Aldrey sp. nov.

urn:lsid:zoobank.org:act:A9C73B13-FA9E-40B0-A90B-B14AF634DE93

Figs 8, 9

Type material.

Holotype.

MEXICO • female; Michoacán state, Acuitzio; 19°26.041'N, 101°17.994'W; 2207 m a.s.l.; 5 Mar. 2018; D. Castillejos-Lemus leg.; ex gall on *Quercus calophylla* (*Quercus* sect. *Lobatae*), insect emerged 5 Apr. 2018; mounted on a card in MNCN.

Paratypes.

MEXICO • 1f; same data as holotype; GenBank: SRX25798192 (individual code Amphibolips_sp_nov_Michoacan231); mounted on stub for SEM observation in ENES-Morelia • 2f; Mexico state, Sultepec; 18°49.856'N, 99°58.088'W; 2381 m a.s.l.; 21 Jun. 2017; D. Castillejos-Lemus leg.; ex gall on *Quercus castanea* (*Quercus* sect. *Lobatae*), insect emerged on 5 Jul. 2017; GenBank: SRX25798236 (individual code Amphibolips_sp_nov_Michoacan_EdM849); 1f mounted on a card in MNCN and 1f preserved in alcohol in ENES-Morelia.

Additional material (only galls).

MEXICO • 5 galls; same data as holotype; 2 dissected and 3 complete; in ENES-Morelia and CNIN • 15 galls; same data as the paratype from Sultepec; 2 dissected and 13 complete; in ENES-Morelia and CNIN • 3 galls; Michoacán state, Villa Madero; 19°24'3.32''N, 101°17'30.56''W; 2120 m a.s.l.; 30 Apr. 2022; D. Castillejos-Lemus leg.; ex gall on *Quercus calophylla* (*Quercus* sect. *Lobatae*); dissected; in ENES-Morelia and CNIN.

Etymology.

Named in honor of Dr. Ken Oyama, a distinguished ecologist renowned for his groundbreaking research on the genus *Quercus*. Dr. Oyama has not only significantly advanced our scientific understanding but has also played a pivotal role in mentoring and inspiring a new generation of Mexican scientists.

Diagnosis.

This species belongs to the same clade as *A. megalokokka*; therefore, its morphological comparisons follow the same framework (see Diagnosis for *A. megalokokka*).

The fore wing pattern of the new species differs from that of all the referenced species. *Amphibolips oyamai* exhibits less pigmentation in the basal and first cubital cells compared to the radial cell and the anterior region of the third cubital cell, where the infuscated band is clearly visible in the other mentioned species (Fig. 9B). However, these cells are slightly more pigmented than the rest of the wing, allowing the general pattern of the clade to be discerned. In the second metasomal tergum, anterior to the area of micropunctures, the area with weak coriaceous-alutaceous sculpture is present, as in other species in this group, but it is much narrower compared to the other species (Fig. 8E). Another characteristic that readily distinguishes this species is its gall morphology (Fig. 9C–E), which is most similar to that of *A. zacatecaensis* among the other species in the clade. However, the gall of *A. oyamai* has a whitish appearance when fresh on the tree (slightly more yellowish in *A. zacatecaensis*), with broad rugosities on the surface that give it a bumpy appearance at some edges (a feature absent in any other known species in this clade), and the texture of the gall is smooth to the touch. Unlike the galls of the other mentioned species, the gall of *A. oyamai* is very soft and can easily tear if not handled carefully when fresh. The epidermis of these galls is very delicate, a characteristic only comparable to the gall of *A. megalokokka*.

Description.

Body length: 5.8 mm (n = 1) for females.

Female (Fig. 9A)**.** Body almost black, but with a less intense black coloration compared to other species. The following structures are chestnut: scape, pedicel, terminal antennal segments, mandibles, metasoma ventrally near the hypopygium (with more extensive reddish coloration that includes the nucha, areas near segment 2 towards the nucha and its lateral parts, the tegula, and areas near the tegula in lateral view), hypopygium, ventral spine, leg joints, tarsomeres, and wing veins (the chestnut color of the wing veins is less evident). Fore wing (Fig. 9B) with a dark band extending along the anterior margin, encompassing the basal cell, first cubital cell, radial cell, and anterior margin and junction with radial cell in the third cubital cell (a faint impression of this dark band visible along the entire margin of the third cubital cell in some specimens, giving it a curved termination at the end). The entire discoidal cell is colorless. In general, the costal cell and anal area are colorless. However, two small regions with very faint spots are visible in the costal cell, near the margin of vein R1+Sc, and in anal area, posterior to vein cu-a.

Head: in dorsal view, 2.25 × wider than long. POL 1.2 × OOL and 2.3 × DOL. Head, in anterior view (Fig. 8A), 1.2 × wider than high; gena slightly broadened behind the eye. Vertex, frons, lower face, and gena with strong reticulate-rugose sculpture; irradiating carinae from clypeus absent; head moderately pubescent, less pubescent on vertex and frons. Clypeus more or less hexagonal, ventral margin strongly projecting over the mandibles and sinuate on anterior margin. Anterior tentorial pits well visible; epistomal sulcus and clypeo-pleurostomal lines weakly indicated. Malar space 0.6 × the height of the compound eye. Toruli situated at mid-height of compound eye; transfacial line 1.35 × the height of an eye; distance between antennal rim and compound eye shorter than the width of torulus including the rim. Ocellar plate raised.

Mouthparts: Mandibles strong and exposed, with dense setae at the base. Cardo of maxilla not visible.

Antenna (Fig. 8B)**:** of moderate length, 0.65 × as long as body length; with 13 antennomeres; flagellum not broadening towards apex; with relatively long, erect setae. Pedicel short, small, broader than long, 0.25 × as long as scape; F1 1.6 × as long as F2. F7–F10 approximately as long as wide; F11 2.5 × as long as wide and 2.2 × as long as F10. Placodeal sensilla present on F3–F11, arranged in dense rows of 5–8 sensilla, confined to dorsal half of each flagellomere.

Mesosoma: in lateral view (Fig. 8F), 1.2 × as long as high. Pronotum pubescent; lateral surface of pronotum with strong, irregular reticulate-rugose sculpture. Pronotum medially short; median pronotal length 0.25 × that of lateral pronotal length. Pronotal plate slightly distinct dorsally.

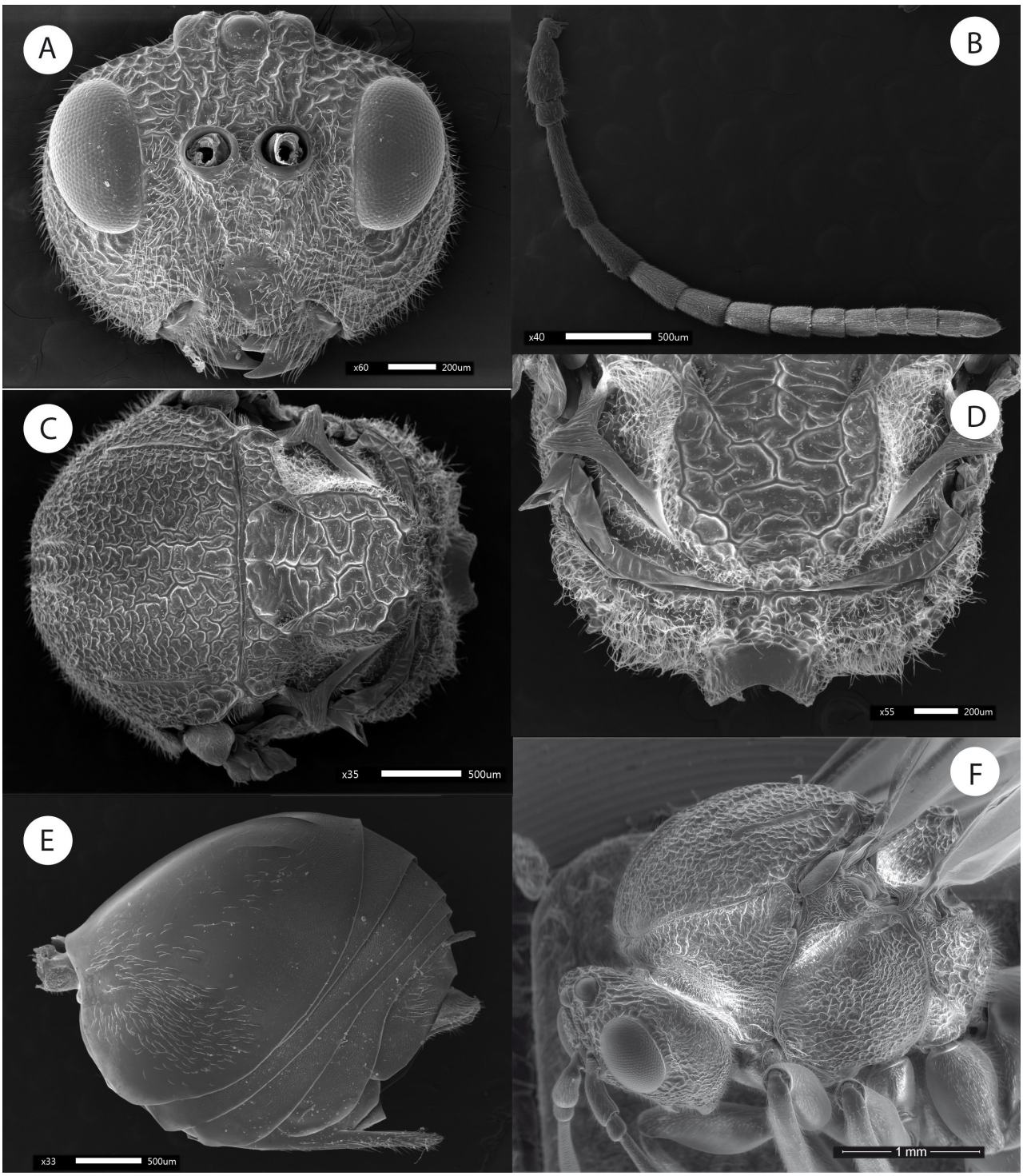

FIGURE 8. *Amphibolips oyamai* sp. nov., female **A** head, anterior view **B** antenna **C** mesosoma, dorsal view **D** mesoscutellum and propodeum **E** metasoma, lateral view **F** mesosoma, lateral view.

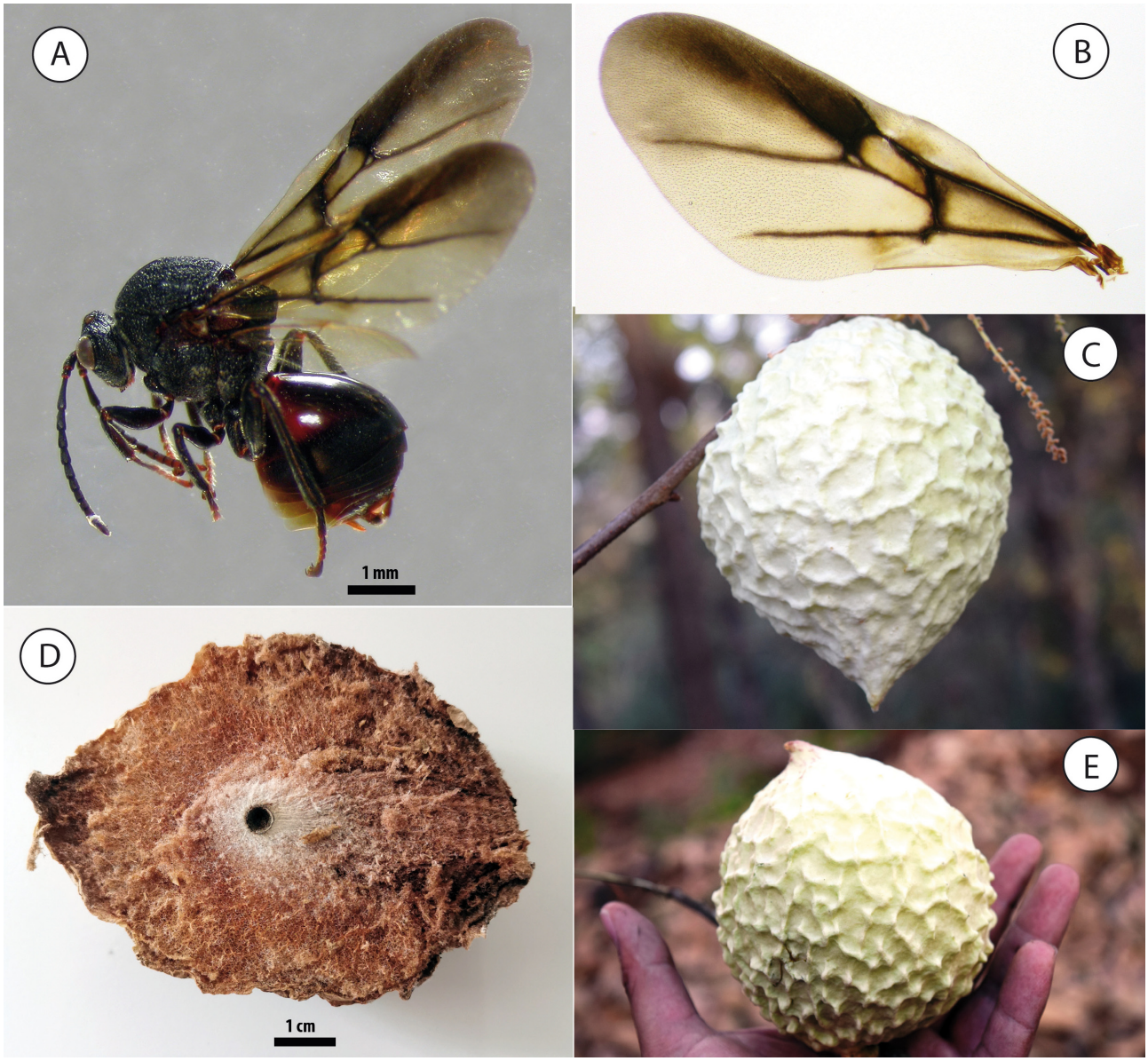

FIGURE 9. *Amphibolips oyamai* sp. nov., female **A** habitus **B** fore wing **C** gall, natural position **D** section of a gall **E** gall.

Mesonotum: Mesoscutum (Fig. 8C, F) pubescent, but setae are short and thin, making them inconspicuous. The sculpture is reticulate-rugose, more pronounced posteriorly; interspaces are smooth and shining, interrupted only by setae, primarily in the anterior part. Notauli obscured by coarse sculpture but discernible in posterior half; strongly convergent posteriorly, a feature which is particularly evident in these specimens. Longitudinal median impression not discernible. Anteroadmedian signa quite visible, extending back to near half of mesoscutum. Parapsidal signa distinct, extending halfway across the mesoscutum. Transscutal fissure narrow, almost straight. Mesoscutellum as long as wide, approximately 0.6 × as long as mesoscutum, rounded posteriorly. Scutellar foveae (Fig. 8C, D) elongated towards the posterior margin, blending homogeneously with the rugose sculpture, giving them a subquadrate appearance; 0.5 × as long as mesoscutellum. A median carina divides the foveae. Sculpture of foveae is smooth with irregular, transverse rugae that increase in prominence towards the posterior margin. Carinae (extensions of these rugae) become very pronounced towards the posterior margin but do not clearly delimit the mesoscutellum. A moderate groove separates the mesoscutellum at the posterior margin. Axillula large, heavily pubescent, with distinct margins. In lateral view, the posterodorsal extension of the body of the subaxillular strip is short, not reaching half the height of the mesoscutellum. Mesopleuron reticulate-rugose, pubescent, with rugae not as strong as those on mesoscutum (Fig. 8F).

Metanotum (Fig. 8D)**:** Metapectal-propodeal complex. Metapleural sulcus reaching posterior margin of mesopectus at approximately mid-height of the metapectal-propodeal complex. Metascutellum somewhat rugose. Metanotal trough pubescent. Median propodeal area with irregular longitudinal and transverse rugae; without pubescence. Lateral propodeal carinae distinct, parallel anteriorly, slightly widening in the posterior half but maintaining the general distance between the carinae at the posterior margin..

Legs: Densely pubescent; femora and tibiae robust. Metatibia 1.5 × as long as metatarsus; apical margin of metatarsomeres 1–4 with long, strong, erect setae. Metatarsal claws featuring prominent triangular basal lobes or teeth.

Fore wing (Fig. 9B)**:** as long as body; radial cell 3.2 × longer than wide; open along anterior margin; areolet present, clearly differentiated. Veins M and Cu1 nearly straight, not reaching wing margin. Rs+M complete, reaching basalis at half its length. First abscissa of radius (2r) curved, not projecting towards the radial cell. Vein Cu1 not branched into two veins. Apical margin with a very short or obsolete hair fringe.

Metasoma (Fig. 8E)**:** in dorsal view, 1.5 × as long as wide; in lateral view, 1.2 × as long as high. Second metasomal tergum covering approximately 0.6 × the length of metasoma; anterior two-thirds smooth and shining, posterior third with a clearly visible band of micropunctures. In the second metasomal tergum, anterior to the area of micropunctures, there is a narrow area with weak coriaceous-alutaceous sculpture, following the anterior smooth area. Punctate sculpture extends onto subsequent terga. Ventral area of second metasomal tergum moderately pubescent. Projecting part of hypopygial spine long; 6.5 × as long as high in lateral view; laterally with long setae, not forming an apical patch.

Variation (Sultepec specimens): The following structures are chestnut: scape, pedicel, mandibles, metasoma ventrally near the hypopygium, hypopygium, ventral spine, leg joints, and only the distal tarsomeres. The terminal antennal segments are not distinctly chestnut, and the chestnut color of the wing veins is more evident than in the Michoacán specimens. The extensive reddish coloration on the nucha, near segment 2, and tegula (as described for the Michoacán population) is absent. Notauli convergent posteriorly (though this convergence is less pronounced than in the Acuitzio specimens). Transscutal fissure slightly sinuate. Mesoscutellum slightly wider than long, approximately 0.6 × as long as mesoscutum. Scutellar foveae deeper, with the median region of the scutellum slightly more elevated; appear elongated laterally with well-defined edges; 0.4 × as long as mesoscutellum. A median carina divides the foveae but is very short and less evident due to the depth and elevation. Sculpture of foveae is smooth with some irregular rugae (not prominently transverse). Axillula with deeper margins. In lateral view, the posterodorsal extension of the body of the subaxillular strip almost extends to the midpoint of the mesoscutellum height. Metascutellum almost smooth and wider than in the Acuitzio specimens. Median propodeal area smoother, with sparse pubescence. Lateral propodeal carinae remaining almost parallel throughout their length. Radial cell 3.5 × longer than wide; areolet completely absent. Projecting part of hypopygial spine 7.5 × as long as high in lateral view.

Gall (Figs 9C–E)**:** Two gall morphologies exist, corresponding to two populations described for this species. Gall of Sultepec paratypes similar to those described for other species of the same clade (TMVB + south SMOc; Castillejos-Lemus *et al*. 2025). Large galls of oak apple type, irregularly spherical with a spongy inner consistency (some slightly elongated towards apex, but those from Sultepec not elongated). Galls from Acuitzio elongated towards apex (similar to gall of *A*. *zacatecaensis*). Difference in Acuitzio galls is that they have pronounced irregularities, which cause deformations on the general surface and form large protuberances in some irregularities. Surface smooth but somewhat rough in Acuitzio galls (due to their broad rugosities), while is smoother in Sultepec galls. They are monothalamic. When fresh, light green in color, but coloration is so faint that they appear whitish on the tree. When fresh, galls can be easily torn by touch, and is common for external texture to be damaged in Sultepec population due to the smaller size of their host species. As is typical for galls of this clade, galls of this species turn light brown when dry. Galls become slightly more resistant to touch when dry. Epidermis is thin, firmly attached to internal spongy tissue when fresh. Internally, spongy tissue occupies the entire space between epidermis and larval chamber. Average diameter of 60 mm and height of 79 mm (diameter ranging from 23 to 81 mm and height from 36 to 115 mm; n = 8) for Acuitzio galls. Average diameter of 45 mm and height of 46 mm (diameter ranging from 30 to 62 mm and height from 29 to 66 mm; n = 15) for Sultepec galls.

Distribution.

Amphibolips oyamai was found in Acuitzio and Villa Madero, in Michoacán state, as well as in Sultepec, Mexico state. Dry galls have also been observed in southern Morelia, Michoacán state (south of Ichaqueo). In all

cases, they occur at elevations above 2000 m a.s.l. It is likely that they exist in additional intermediate locations at high elevations.

Biology.

Only females are known for this species. Galls from Acuitzio develop on *Quercus calophylla*, while those from Sultepec develop on *Q. castanea*. In both cases occur above 2100 m a.s.l. Galls from Michoacán state were collected in March, and insects emerged in April. In some localities, Michoacán galls may be found on the same host trees as those of *A. chilito*. Galls from Mexico state were collected in June, and insects emerged in July.

Remarks.

This wasp is assigned to the TMVB + south SMOc clade (as defined in Castillejos-Lemus *et al*. 2025).

Amphibolips idiopteryx Nieves-Aldrey & Castillejos-Lemus sp. nov.

urn:lsid:zoobank.org:act:946FB54B-350B-4CC2-99FB-2FD2649C09AA

Figs 10–12

Type material.

Holotype.

MEXICO • female; Oaxaca state, San Pedro Yaneri, San Juan Tepanzacoalco; 17°23.992'N, 96°23.792'W; 1784 m a.s.l.; 19 Apr. 2018; D. Castillejos-Lemus leg.; ex gall on *Quercus scytophylla* (*Quercus* sect. *Lobatae*), insect emerged on 17 May 2018; mounted on a card in MNCN.

Paratypes.

MEXICO • 2m; same data as holotype; mounted on cards in MNCN • 1m; same data as holotype; GenBank: SRX25798190 (individual code Amphibolips_sp_nov2_Oaxaca_252); mounted on stubs for SEM observation in ENES-Morelia • 1f; Oaxaca state, San Andrés Yaá; 17°17.415'N, 96°07.979'W; 1723 m a.s.l.; 24 Apr. 2018; D. Castillejos-Lemus leg.; ex gall on *Quercus* sp, insect emerged on 3 May 2018; mounted on card in MNCN.

Additional material (only galls).

MEXICO • 19 galls; same data as holotype; 4 dissected and 15 complete; in ENES-Morelia and CNIN.

Etymology.

The epithet *idiopteryx* derives from the Greek *idios* (ἴδιος) meaning "peculiar" or "distinct", and *pteryx* (πτέρυξ), meaning "wing". The name refers to the unique fore wing morphology of this species.

Diagnosis.

This species belongs to the group characterized by the presence of a dark, heavily infuscated band along the anterior region of the fore wing from Oaxaca (*A. idiopteryx*, *A. zapoteco* and *A. darioi*). Based on their geographical distribution and wing spot patterns, *A. oaxacae* likely belongs to the same clade. The affinity of *A. nigrialatus* is difficult to assign due to its absence in the phylogenetic study and its unique wing spot pattern. However, based on morphological and geographical evidence, we concluded that *A. idiopteryx* belongs to this clade.

Amphibolips idiopteryx differs from *A. zapoteco*, as follows: the clear spot in the third cubital cell, present (Fig. 12C); the proportion of smooth and shining areas on second metasomal tergum, greater (1/3); smooth depression below eyes, absent; pedicel longer relative to scape; malar space relative to the height of an eye, smaller; scutellar fovea relatively square and separated by a carina (Fig. 10C, D); white coloration is usually predominant in mature galls of *A. idiopteryx*, whereas galls of *A. zapoteco* tend to be greener when mature. It differs from *A. darioi* as follows: vein R1 in radial cell, present; pigmentation of anal and basal cells, more evident in *A. idiopteryx* (Fig. 12C); unpigmented spot in third cubital cell always present; galls with pointed protuberances, evident (Fig. 12F); white spots on gall surface evident; proportion of smooth and shining areas on second metasomal tergum, greater (1/3); two longitudinal carinae on face, absent; mesoscutellar groove, stronger (Fig. 10B–D). It differs from *A. oaxacae* as follows: pigmentation of anal cell, not restricted to proximal half; unpigmented spot in third cubital cell always present (Fig. 12C); basal cell of *A. oaxacae* lacks unpigmented spots (Fig. 18F); galls with pointed protuberances, evident; proportion of smooth and shining areas on second metasomal tergum, smaller, and coriaceous-alutaceous sculpture, absent in *A. oaxacae*. It differs from *A. nigrialatus* as follows: *A. nigrialatus* has a generally darker coloration of fore wing; clear spot in *A. idiopteryx* restricted to third cubital cell (Fig. 12C), whereas in *A. nigrialatus*, this spot extends from third cubital cell to the discoidal cell (Fig. 18B); areolet present, absent in *A. nigrialatus*; galls with pointed protuberances, evident (Fig. 12F); white spots on gall surface evident;

proportion of smooth and shining areas on second metasomal tergum, smaller, 1/2 in *A*. *nigrialatus*; two longitudinal carinae on face are absent; malar space relative to the height of an eye, smaller.

Description.

Body length: 6.1 mm (n = 2) for females.

Female (Fig. 12A)**:** Body almost black, particularly intense on the thorax, head, posterior part of metasoma, and first segments of legs. Distal part of antennal scape and pedicel usually have a chestnut region. Last flagellomeres chestnut ventrally and black dorsally. Mandibles chestnut. Tarsi typically range from light brown to dark brown from the anterior to posterior part. Metasoma slightly chestnut ventrally. First metasomal tergum and immediate anterior region of second metasomal tergum, near the first metasomal tergum, chestnut. Hypopygium and areas near hypopygium and ventral spine, chestnut, lighter on ventral spine. Fore wing (Fig. 12C) with a dark band extending along anterior margin, encompassing the basal cell, first cubital cell, radial cell, costal cell, and anterior margin and junction with the radial cell in the third cubital cell. Most of the discoidal cell, colorless, except for the wing margin, which has a faint dark band. Costal cell has a less intensely pigmented area at the junction of vein Rs with vein R+Sc, extending towards the anterior margin of wing. Anal cell, usually colorless across most of its extent but exhibits two more heavily pigmented spots on the posterior margin of wing. The first basally positioned, before vein cu-a, apparently delimited anteriorly by vein 1A. The second spot is at the posterior margin (posterior to vein cu-a) and continues with the pigmented band of discoidal cell. Veins R+Sc, Rs, M, and the first half of R1, black. Remaining veins are chestnut or brown. Vein Rs+M has one-third of its length unpigmented at its junction with vein M. Veins M (at the margin of the third cubital cell) and Cu1, light brown, are usually the lightest compared to other wing veins. In the distal third or third cubital cell, there is an unpigmented region that does not interrupt the anterior band but is highlighted by pigmentation of the distal region of the cell surrounding it.

Head: in anterior view (Fig. 11A), 1.2 × wider than high; gena slightly broadened behind the eye. Vertex, frons, lower face, and gena with strong reticulate-rugose sculpture. Irradiating carinae from the clypeus, absent. Head moderately pubescent, less pubescent on vertex and frons (Fig. 10A, C, F). Clypeus more or less hexagonal, ventral margin strongly projecting over mandibles and sinuate on anterior margin. Anterior tentorial pits well visible; epistomal sulcus and clypeo-pleurostomal lines, weakly indicated. Malar space 0.6 × the height of the compound eye. Toruli situated at mid-height of the compound eye. Transfacial line 1.5 × the height of an eye. Distance between antennal rim and compound eye, shorter than the width of the torulus including the rim. Ocellar plate slightly raised.

Mouthparts: Mandibles strong and exposed, with dense setae at the base. Cardo of maxilla not visible. Apical peg of the last maxillary segment present.

Antenna (Fig. 10A)**:** of moderate length, 0.5 × as long as body length; with 13 antennomeres. Flagellum not broadening towards apex, with short and erect setae. Pedicel short, small, as broad as long, 0.4 × as long as scape. F1 1.7 × as long as F2. F7–F10 approximately as long as wide. Placodeal sensilla present on F3–F11, arranged in dense rows of sensilla from F4 onwards, confined to the ventral half of each flagellomere.

Mesosoma: in lateral view (Fig. 10B, F), 1.15 × as long as high. Pronotum pubescent; lateral surface of pronotum with strong, irregular reticulate-rugose sculpture. Pronotum, medially short but slightly larger than in other species; median pronotal length 0.3 × that of lateral pronotal length. Pronotal plate slightly distinct dorsally.

Mesonotum: Mesoscutum (Fig. 10B–D, F) pubescent, primarily in the anterior part, but setae are very short and thin, making them conspicuous only in the anterior region near the pronotum. The sculpture is reticulate-rugose, with smooth and shining interspaces. Notauli not discernible. Longitudinal median impression barely perceptible, only near the transscutal fissure. Anteroadmedian signa quite visible, extending back to near the midpoint of mesoscutum. Parapsidal signa obscured by sculpture but discernible up to the midpoint of mesoscutum. Transscutal fissure narrow, slightly sinuate. Mesoscutellum as wide as long, approximately 0.5 × as long as mesoscutum. Strongly coarsely rugose, pubescent, with a broad median longitudinal impression that makes mesoscutellum emarginate posteriorly (Fig. 10B–D); median longitudinal impression extends anteriorly to scutellar foveae. Scutellar foveae (Fig. 10D) 0.45 × as long as mesoscutellum, relatively square and deep, almost without pubescence, separated by a carina. With usually transverse rugae of variable length and smooth interspaces. Axillula, large, pubescent, but setae are small and sparse, not very deep, and with posterior margin not delimited. In lateral view, the posterodorsal extension of the body of the subaxillular strip reaches half the height of mesoscutellum. Mesopleuron reticulate-rugose, pubescent, with rugae not as strong as those on mesoscutum (Fig. 10F). Posterior groove of the mesopleural triangle present below the tegula but shallow.

Metanotum: Metapectal-propodeal complex. Metapleural sulcus reaching the posterior margin of mesopectus at approximately mid-height of metapectal-propodeal complex. Metascutellum slightly rugose and shiny. Metanotal trough pubescent. Propodeal area with irregular rugae, with pubescence primarily on sides; lateral propodeal carinae barely distinct due to the rugae, but the sparse pubescence allows this area to be visible.

Legs: Densely pubescent, particularly on tibiae and tarsi; femora and tibiae robust. Metatibia 1.7 x as long as metatarsus; apical margin of metatarsomeres 1–4 with long, strong, erect setae. Metatarsal claws with prominent triangular basal lobes or teeth.

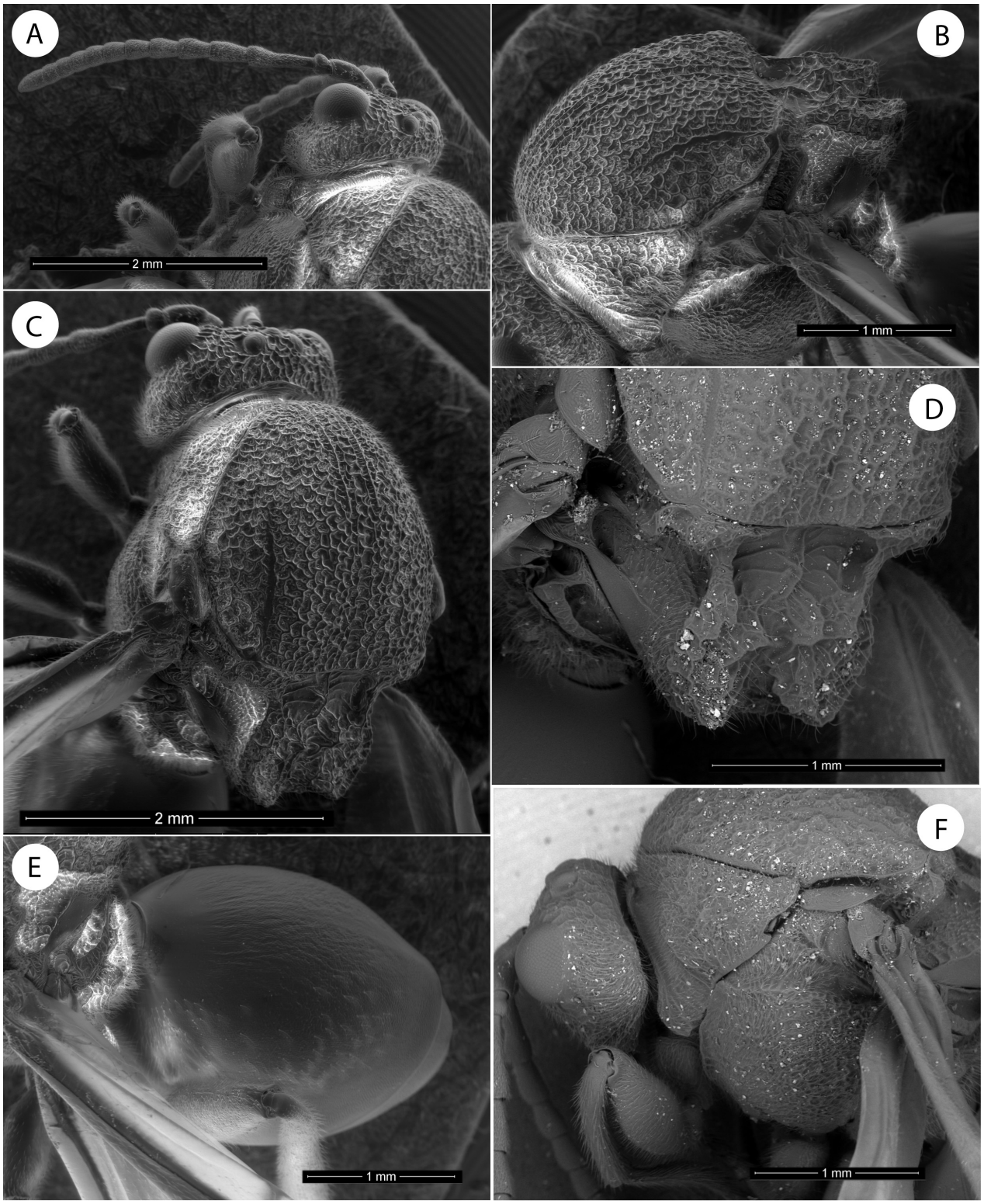

FIGURE 10. *Amphibolips idiopteryx* sp. nov., female **A** antenna and head in dorsolateral view **B** mesosoma, dorsolateral view **C** head and mesosoma, dorsal view **D** mesoscutellum **E** metasoma, dorsal view **F** mesosoma, lateral view.

FIGURE 11. *Amphibolips idiopteryx* sp. nov., male **A** head, anterior view **B** antenna **C** mesosoma, dorsal view **D** detail of basal antennomeres **E** leg **F** mesosoma, lateral view.

Fore wing (Fig. 12C)**:** slightly longer than the body. Radial cell 3.2 × longer than wide; open along anterior margin. Areolet present. Veins M and Cu1 nearly straight, not reaching wing margin. Rs+M complete, reaching basalis at half its length, but half of its length unpigmented at its junction with vein M. First abscissa of radius (2r) curved, slightly projecting towards the radial cell. Vein Cu1 not branched into two veins. Apical margin with a very short or obsolete hair fringe. In the distal third of the third cubital cell, there is an unpigmented region that does not interrupt the anterior band but is highlighted by pigmentation of the distal region of the cell surrounding it. Most densely pigmented regions are the basal cell, distal half of the radial cell, and area of the third cubital cell near the radial cell.

Metasoma (Fig. 10E)**:** in lateral view, 1.3 × as long as high. Second metasomal tergum covering approximately 0.6 × the length of metasoma; anterior one-third smooth and shining, posterior third with a clearly visible band of micropunctures. In the second metasomal tergum, anterior to the area of micropunctures, there is an area with coriaceous-alutaceous sculpture extending to sides, following the anterior smooth area. Punctate sculpture extends onto subsequent terga. Ventral area of second metasomal tergum moderately pubescent. Projecting part of hypopygial spine long; 7.8 × as long as high in lateral view; ventrally tapering in width towards apex, laterally with long setae, not forming an apical patch.

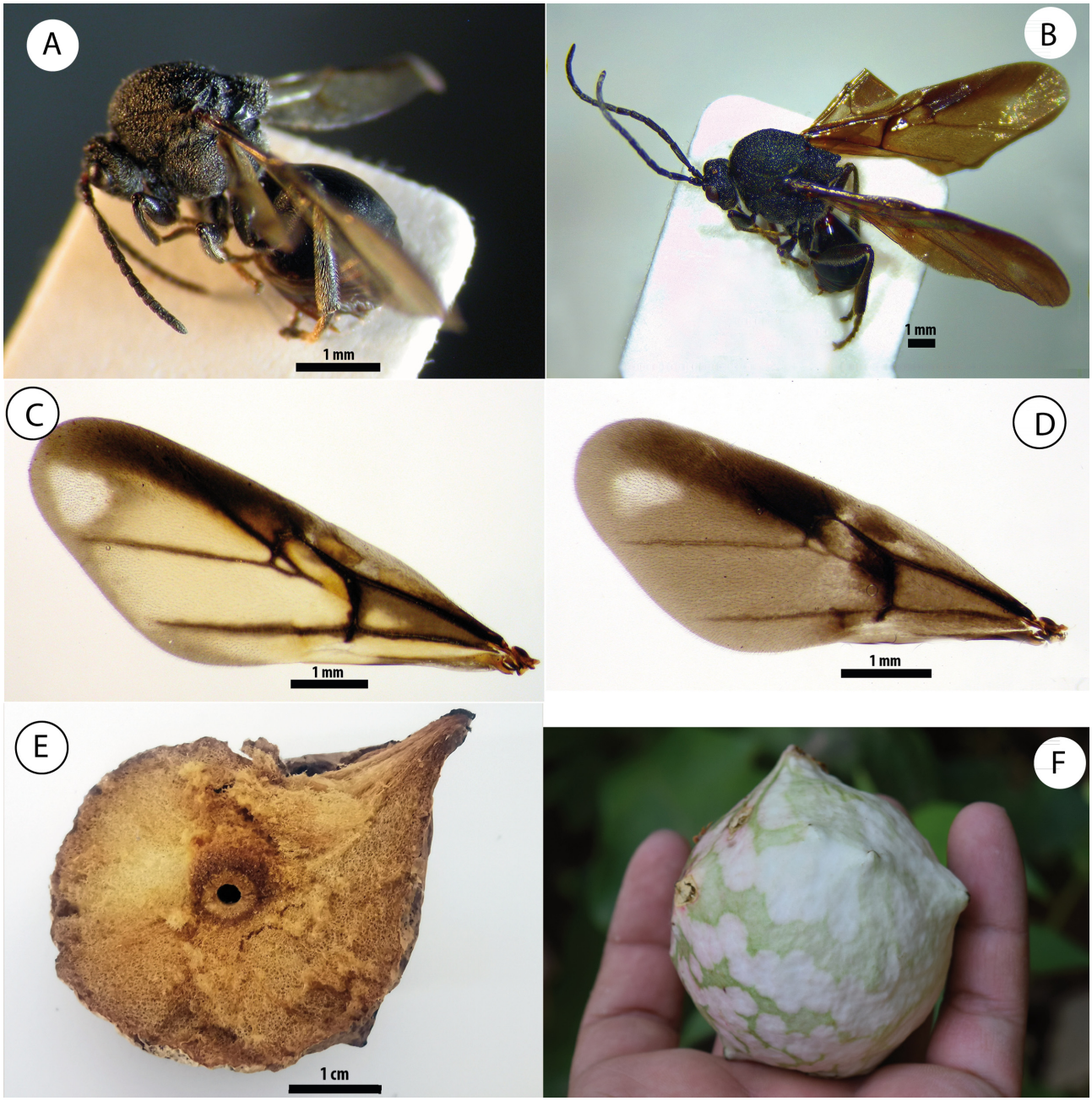

FIGURE 12. *Amphibolips idiopteryx* sp. nov. **A** female habitus **B** male habitus **C** female fore wing **D** male fore wing **E** section of a gall **F** gall.

Male (Fig. 12B)**:** Differs from female as follows: 5.1 mm (n = 3). Metasoma smaller than thorax (contrary in females). Antennae, legs, and wings longer relative to the body. Antennae with 15 antennomeres (Fig. 11B); F1 slightly modified (Fig. 11D), flattened on ventral side, with elongate placodeal sensillae visible in all flagellomeres. Mesoscutellum more widely and deeply emarginated on posterior margin (Fig. 11C). Posterodorsal extension of the body of the subaxillular strip slightly shorter (Fig. 11F). Metatibia 1.4 × as long as metatarsus (Fig. 11E). Fore wings more heavily infuscate across their entire surface, but darker anterior band and unpigmented regions remain visible, retaining the same pattern as in female (Fig. 12D). Unpigmented region at the end of the third cubital cell, more reduced. Proximal half of the first cubital cell, as intensely pigmented as the radial cell, both darker than basal cell.

Gall (Fig. 12E, F)**:** Galls are relatively spherical, with some protuberances (which may vary in size) randomly scattered across the smooth surface of the gall. Protuberances are less numerous and larger than in *A*. *cibriani* Pujade-

Villar, 2018, and less pronounced and scattered than in *A*. *oyamai*. The surface is smooth, somewhat sticky, and firm to the touch. They are monothalamic. When fresh, the surface is green and white in color. There is no defined pattern in coloration; it appears as a somewhat random mixture of patches of two colors. Galls turn light brown when dry, but the white spots on gall surface remain visible, and they become more fragile to the touch. The epidermis is thin, firmly attached to internal spongy tissue when fresh. Internally, spongy tissue occupies the entire space between epidermis and larval chamber. Average longitudinal diameter is 4.7 cm, and average transversal diameter is 4 cm (longitudinal diameter ranging from 20 to 63 mm and transversal diameter from 19 to 54 mm; n = 19).

Distribution.

Amphibolips idiopteryx was found in San Juan Tepanzacoalco and San Andrés Yaá, in Northern Oaxaca state, at an altitude of between 1723 and 1784 m a.s.l. The approximate linear distance between the two sites is 28 km. Both locations belong to the Papaloapan hydrological basin.

Biology.

Only sexual generation is known. Smaller galls are typically those that do not yield adult *Amphibolips* due to parasitoid attacks or presence of inquilines. As a result, the average measurements of galls are influenced by these factors (we excluded five smallest galls from the average). Galls were collected in April, and insects emerged in May.

Remarks.

This species belongs to the Oaxaca clade (as defined in Castillejos-Lemus *et al*. 2025),

Amphibolips zapoteco **Nieves-Aldrey & Castillejos-Lemus sp. nov.**

urn:lsid:zoobank.org:act:49522F2D-070C-42BF-9C60-6DB9103135C1

Figs 13–15

Type material.

Holotype.

MEXICO • female; Oaxaca state, San Pablo Macuiltianguis; 17°32.296’N, 96°33.483’W; 2172 m a.s.l.; 20 Apr. 2018; D. Castillejos-Lemus leg.; ex gall on *Quercus* sp (*Quercus* sect. *Lobatae*), insect emerged on 30 Apr. 2018; mounted on a card in MNCN.

Paratypes.

MEXICO • 1f 4m; same collection location; ex gall on *Quercus crassifolia* (*Quercus* sect. *Lobatae*), insects emerged on the same date and in 3 May 2018; GenBank: SRX25798212 (individual code Amphibolips_sp_nov3_Oaxaca_259); 1f 1m mounted on a stub for SEM observation at MNCN, 1m mounted on a card in MNCN, 1m mounted on a card in ENES-Morelia, 1m in alcohol in ENES-Morelia (extracted dead from the gall on 6 Dec. 2024) • 3f; same collection location; 17°32.397’N, 96°31.839’W; 2466 m a.s.l.; 26 Mar. 2017; D. Castillejos-Lemus leg.; ex gall on *Quercus* sp (*Quercus* sect. *Lobatae*), insects emerged on 4–5 Apr. 2017; 1f mounted on a card in MNCN, 2f in ENES-Morelia, one mounted on a card and the other preserved in alcohol • 1f; Oaxaca state, Santa María Jaltianguis; 17°21.506’N, 96°31.248’W; 2326 m a.s.l.; 26 Mar. 2017; D. Castillejos-Lemus leg.; ex gall on *Quercus scytophylla* (*Quercus* sect. *Lobatae*), insect emerged on 4 Apr. 2017; GenBank: SRX25798213 (individual code Amphibolips_sp_nov3_Oaxaca_365); mounted on a card in ENES-Morelia • 1f; Oaxaca state, Ixtlán de Juárez; 17°19.316’N, 96°28.197’W; 2230 m a.s.l.; 25 Mar. 2017; D. Castillejos-Lemus leg.; ex gall on *Quercus crassifolia* (*Quercus* sect. *Lobatae*), insect emerged on 24 Apr. 2017; GenBank: SRX25798219 (individual code Amphibolips_sp_nov3_Oaxaca_353); mounted on a card in MNCN • 2f; Oaxaca state, Santiago Comaltepec; 17°33.116’N, 96°33.923’W; 2145 m a.s.l.; 22 Apr. 2018; D. Castillejos-Lemus leg.; ex gall on *Quercus elliptica* (*Quercus* sect. *Lobatae*), insect emerged on 30 Apr. 2018; GenBank: SRX25798215 (individual code Amphibolips_sp_nov3_Oaxaca_294_2); 1f mounted on a card in MNCN and 1f preserved in alcohol in ENES-Morelia • 1f; Oaxaca state, Santiago Comaltepec; 17°33.537’N, 96°33.391’W; 2051 m a.s.l.; 22 Apr. 2018; D. Castillejos-Lemus leg.; ex gall on *Quercus* sp (*Quercus* sect. *Lobatae*), insect emerged on 30 Apr. 2018; mounted on a card in ENES-Morelia (remains of another individual extracted dead from its gall and preserved in alcohol on 9 Dic. 2024) • 1m; Oaxaca state, Santiago Comaltepec; 17°33.502’N, 96°33.199’W; 2077 m a.s.l.; 26 Mar. 2017; D. Castillejos-Lemus leg.; ex gall on *Quercus scytophylla* (*Quercus* sect. *Lobatae*), insect emerged on 4 Apr. 2017; mounted on a card in ENES-Morelia • 1m; Oaxaca state, Santiago Comaltepec; 17°33.494’N, 96°32.244’W; 2351 m a.s.l.; 22 Apr. 2018; D. Castillejos-Lemus leg.; ex gall on *Quercus* sp (*Quercus* sect. *Lobatae*), insect emerged on 30 Apr. 2018;

mounted on a card in MNCN • 1f; Oaxaca state, San Juan Quiotepec; 17°35.055'N, 96°34.960'W; 2123 m a.s.l.; 26 Mar. 2017; D. Castillejos-Lemus leg.; ex gall on *Quercus crassifolia* (*Quercus* sect. *Lobatae*), insect emerged on 17 Apr. 2017; GenBank: SRX25798214 (individual code Amphibolips_sp_nov3_Oaxaca_Q3); mounted on a card in ENES-Morelia • 3m; Oaxaca state, Santiago Comaltepec; 17°33.402'N, 96°33.819'W; 2066 m a.s.l.; 22 Apr. 2018; D. Castillejos-Lemus leg.; ex gall on *Quercus* x *dysophylla* (*Quercus* sect. *Lobatae*), insects emerged on 30 Apr.–1 May 2018; GenBank: SRX25798191 (individual code Amphibolips_sp_nov3_Oaxaca_293_2); 2m mounted on a card in MNCN and 1m preserved in alcohol in ENES-Morelia • 1f; Oaxaca state, San Juan Quiotepec; 17°35.003'N, 96°34.964'W; 2099 m a.s.l.; 26 Mar. 2017; D. Castillejos-Lemus leg.; ex gall on *Quercus scytophylla* (*Quercus* sect. *Lobatae*), insect emerged on Apr/17/2017; mounted on a card in MNCN.

Additional material (only galls).

MEXICO • 40 galls; same data as the paratype from 2172 m a.s.l.; 3 dissected and 37 complete; in ENES-Morelia and CNIN • 8 galls; same data as the paratype from 2466 m a.s.l.; 2 dissected and 6 complete; in ENES-Morelia and CNIN • 7 galls; same data as holotype; 3 dissected and 4 complete; in ENES-Morelia and CNIN • 8 galls; same data as the paratype from 2051 m a.s.l.; 2 dissected and 6 complete; in ENES-Morelia and CNIN • 5 galls; same data as the paratype from 2351 m a.s.l.; 2 dissected and 3 complete; in ENES-Morelia and CNIN • 17 galls; same data as the paratype from 2066 m a.s.l.; 3 dissected and 14 complete; in ENES-Morelia and CNIN • 14 galls; same data as the paratype from 2145 m a.s.l.; 2 dissected and 12 complete; in ENES-Morelia and CNIN.

Etymology.

The specific epithet "*zapoteco*" refers to the Zapoteco people, an indigenous group native to the region of Mexico where this species was discovered. The name honors their rich cultural and historical heritage, as well as their deep connection to the natural landscapes of the area.

Diagnosis.

Amphibolips zapoteco will be compared with other species from Oaxaca, following the same approach used for *A. idiopteryx* (see diagnosis of *A. idiopteryx*).

Amphibolips zapoteco differs from *A. idiopteryx*, as follows: clear spot in the third cubital cell, absent (Fig. 15C); proportion of smooth and shining areas on the second metasomal tergum, smaller (1/5); smooth depression below eyes, present (Fig. 13A); pedicel shorter relative to scape (0.25), broader than long (Fig. 13C); malar space relative to the height of an eye, larger; scutellar fovea ovoid and not separated by a carina (Fig. 13B). It differs from *A. darioi* as follows: vein R1 in the radial cell, present; clear spot in the third cubital cell, absent; pigmentation of the basal cell, more evident in *A. zapoteco*; galls with pointed protuberances, evident (Fig. 15E); white spots on gall surface, evident; two longitudinal carinae on face, absent; smooth depression below eyes, present; pedicel shorter relative to scape (0.25), broader than long; malar space relative to the height of an eye, larger; scutellar fovea ovoid and not separated by a carina; mesoscutellar groove, deeper and broader. It differs from *A. oaxacae* as follows: pigmentation of anal cell, not restricted to the proximal half; galls with pointed protuberances, evident; proportion of smooth and shining areas on the second metasomal tergum, smaller, and coriaceous-alutaceous sculpture, absent in *A. oaxacae*; smooth depression below eyes, present; pedicel shorter relative to scape (0.25), broader than long; malar space relative to the height of an eye, larger; scutellar fovea ovoid and not separated by a carina. It differs from *A. nigrialatus* as follows: *A. nigrialatus* has a generally darker coloration of the fore wing; clear spot in *A. zapoteco*, absent in the third cubital cell, whereas in *A. nigrialatus*, this spot extends from the third cubital cell to discoidal cell (Fig. 18B); areolet present, absent in *A. nigrialatus*; galls with pointed protuberances, evident; white spots on gall surface, evident; proportion of smooth and shining areas on the second metasomal tergum, smaller, 1/2 in *A. nigrialatus*; two longitudinal carinae on face, absent; smooth depression below eyes, present; pedicel shorter relative to scape (0.25), broader than long; scutellar fovea ovoid.

Description.

Body length: 5.7 mm average (n = 4; 5.4 mm / 5.8 mm) for females.

Female (Fig. 15A)**:** Body almost entirely black. Basal and distal parts of the antennal scape and pedicel usually have a chestnut region. In some individuals, the last flagellomeres chestnut ventrally and black dorsally. Mandibles chestnut. Mesosoma entirely black. Tarsi dark brown. Metasoma black dorsally and chestnut ventrally. First metasomal tergum and immediate anterior region of the second metasomal tergum, near the first metasomal tergum, yellowish, giving the appearance of a ring alongside first metasomal tergum. Posterior margins of metasomal terga, posterior to the bands of micropunctures, chestnut. Hypopygium and areas near hypopygium and ventral spine, chestnut, lighter on ventral spine, almost yellow. Fore wing (Fig. 15C) with a dark band extending along anterior margin, encompassing the basal cell, first cubital cell, radial cell, half of the costal cell (adjacent to first cubital

cell), and anterior margin and junction with the radial cell in the third cubital cell. Entire discoidal cell is colorless, but some darker specimens have slight pigmentation along the margin of vein Cu1 at mid-length. Anal cell, usually colorless across most of its extent but exhibits two more heavily pigmented spots on the posterior margin of wing. The first, basally positioned, before vein cu-a, apparently delimited anteriorly by vein 1A. The second spot, at the posterior margin (posterior to vein cu-a) but does not extend towards the discoidal cell. Almost all veins are chestnut or unpigmented at the center. Darkest veins are the proximal half of R+Sc and veins Rs and M, which delimit basal cell, but in general, veins visible because exhibit some degree of color loss.

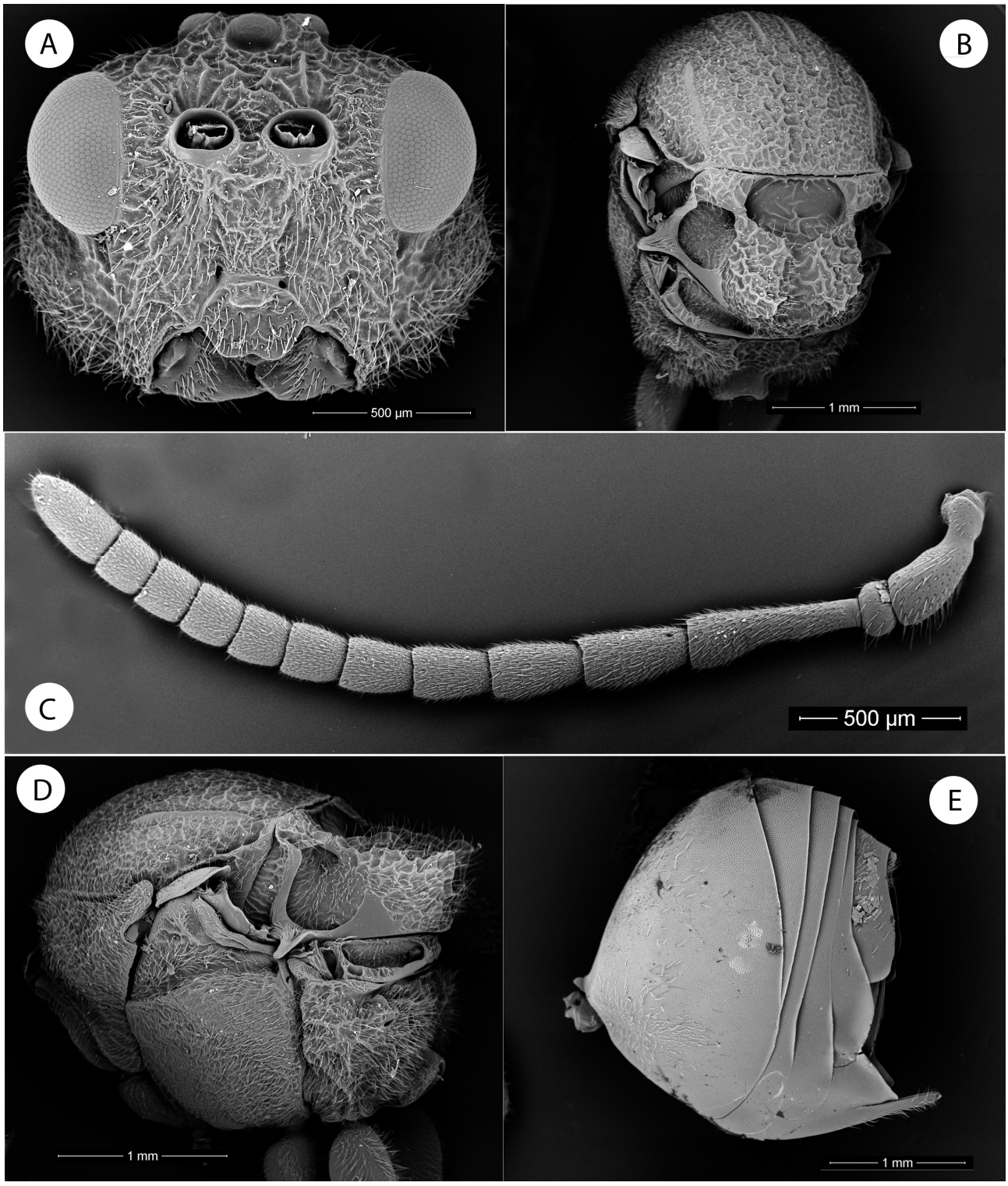

FIGURE 13. *Amphibolips zapoteco* sp. nov., female **A** head, anterior view **B** mesosoma, dorsal view **C** antenna **D** mesosoma, lateral view **E** metasoma, lateral view.

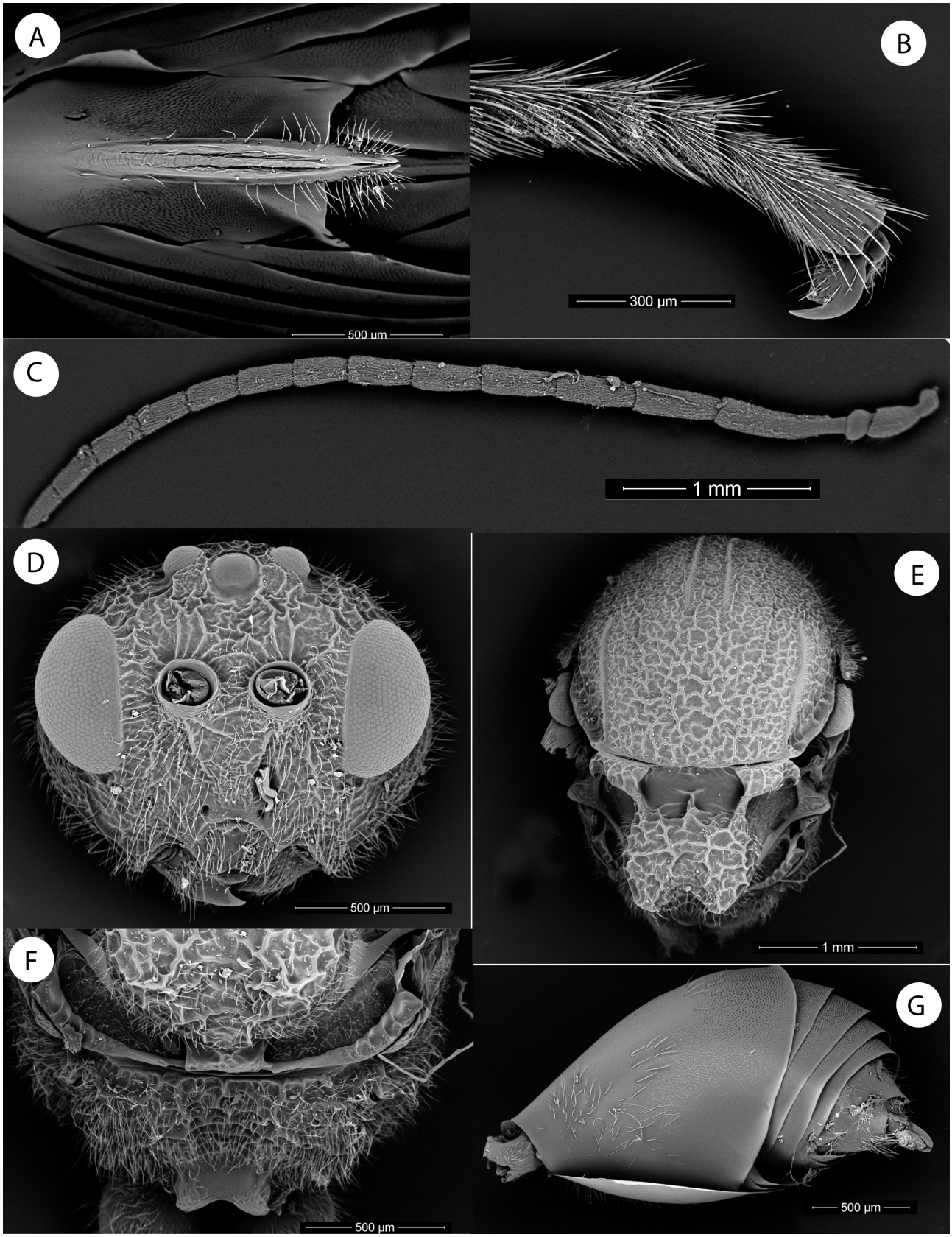

FIGURE 14. *Amphibolips zapoteco* sp. nov. **A** female hypopygium, ventral view **B** female metatarsal claw **C** male antenna **D** male head, anterior view **E** male mesosoma, dorsal view **F** male metascutellum and propodeum **G** male metasoma, lateral view.

Head: in dorsal view, 2.3 × wider than long. POL 0.9 × OOL and 2 × DOL. Head, in anterior view (Fig. 13A), 1.25 × wider than high; gena slightly broadened behind the eye. Vertex, frons, lower face, and gena with strong reticulate-rugose sculpture. Irradiating carinae from clypeus absent. Head moderately pubescent, less pubescent on vertex and frons. Clypeus more or less hexagonal, ventral margin strongly projecting over mandibles and sinuate on anterior margin. Anterior tentorial pits, well visible; epistomal sulcus and clypeo-pleurostomal lines, weakly indicated. Small protuberance present above the epistomal sulcus. Malar space 0.75 × the height of the compound eye. Toruli situated at mid-height of the compound eye. Transfacial line 1.6 × height of an eye. Distance between antennal rim and compound eye, shorter than the width of the torulus including rim. Ocellar plate slightly raised. Below the eye, there is a region with fewer rugosities, which in some specimens appears as a depression extending towards mandibles.

Mouthparts: Mandibles, strong and exposed, with dense setae in base.

Antenna (Fig. 13C)**:** of moderate length, 0.6 × body length; with 13 antennomeres. F10 and F11, distinctly separated. Flagellum not broadening towards apex, with short and erect setae. Pedicel short and small, 1.6 × wider than long, and 0.25 × length of the scape. F1 1.6 × as long as F2. F7–F10 appear approximately as long as wide. F11 1.5 × as long as wide and twice as long as F10. Placodeal sensilla present on F3–F11, arranged in dense rows starting from F4, confined to the ventral half of each flagellomere.

Mesosoma: in lateral view (Fig. 13D), 1.2 × as long as high. Pronotum pubescent; lateral surface of pronotum with strong, irregular, reticulate-rugose sculpture. Pronotum, medially short, though slightly larger than in other species; median pronotal length 0.35 × that of lateral pronotal length. Pronotal plate slightly distinct dorsally. Central region of pronotum, smooth and shiny, quite conspicuous and broad compared to the rest of pronotum, which exhibits rugosities and pubescence; however, pubescence also present along edges within the shiny area.

Mesonotum: Mesoscutum (Fig. 13B) pubescent, primarily in the anterior region, but setae very short and thin, conspicuous only in anterior area near the pronotum. Sculpture, reticulate-rugose; interspaces, smooth and shining, interrupted only by the setae in the anterior region or by the reduced size of reticulae. Notauli not discernible. Longitudinal median impression barely perceptible, only noticeable next to the transscutal fissure. Anteroadmedian signa obscured by sculpture but still visible, extending backward to just before the midpoint of mesoscutum. Parapsidal signa obscured by sculpture but discernible up to mid-length of mesoscutum. Transscutal fissure narrow, almost straight, slightly sinuate. Mesoscutellum as wide as long, approximately 0.5 × as long as mesoscutum. Strongly and coarsely rugose, slightly pubescent, with a broad median longitudinal impression that makes the mesoscutellum emarginate posteriorly (Fig. 13B); median longitudinal impression extends anteriorly to scutellar foveae and shares the same internal sculpture as foveae, appearing as an extension of foveae. Scutellar foveae (Fig. 13B) 0.4 × as long as mesoscutellum, ovoid, relatively deep, lacking pubescence, and fused, not separated by a carina. With sparse rugae, generally transverse, well-separated, and of variable length; interspaces smooth. Axillula large, pubescent, and rugose, with shining interspaces, not very deep, and with the posterior margin not delimited. In lateral view, posterodorsal extension of the body of the subaxillular strip reaches half the height of mesoscutellum. Mesopleuron reticulate-rugose, pubescent, with rugae similar to those of mesoscutum (Fig. 13D). Mesopleural triangle, slightly shinier than the rest of mesopleuron. Posterior groove of the mesopleural triangle, present below tegula, with very faint rugae, shiny (similar to deeper region of mesopleural triangle that borders the rest of mesopleuron), and anteriorly delimited by a small carina.

Metanotum (Fig. 14F)**:** Metapectal-propodeal complex. Metapleural sulcus reaching the posterior margin of mesopectus at approximately mid-height of metapectal-propodeal complex. Metascutellum rugose and slightly shiny. Metanotal trough pubescent and smooth, relatively shallow. Propodeal area with irregular rugae; pubescence present, primarily on sides. Lateral propodeal carinae, indistinct due to rugae, but the reduced pubescence and a slight depression allow this area to be distinguished.

Legs: Densely pubescent, particularly on tibiae and tarsi; femora and tibiae robust. Metatibia 1.65 × as long as metatarsus; apical margin of metatarsomeres 1–4 with long, strong, erect setae. Metatarsal claws with strong, triangular basal lobes or teeth (Fig. 14B).

Fore wing (Fig. 15C)**:** 1.2 × as long as the body. Radial cell, approximately 3.25 × longer than wide; open along the anterior margin, including the strong reduction in length of vein R1 (primarily visible due to the extension of pigmentation). Areolet present, although vein M in this cell may appear diffuse due to loss of pigmentation. Veins M and Cu1 nearly straight, not reaching wing margin. Rs+M complete, reaching basalis at mid-length, but approximately a quarter of its length lacks pigmentation near its junction with vein M. First abscissa of radius (2r)

curved, slightly projected towards the radial cell. Vein Cu1, not branched into two veins, but exhibits a pigmented spot in the hypothetical region of vein Cu1b, which in some specimens extends to the margin of anal cell. Apical margin with very short or obsolete hair fringe. Most densely pigmented regions are the radial cell, first cubital cell, and basal cell.

Metasoma (Fig. 13E)**:** in dorsal view 1.6 × as long as wide; in lateral view, as long as high. Second metasomal tergum covering approximately 0.6 × the length of metasoma; anterior one-fifth smooth and shining, posterior third with a band of micropunctures clearly visible. Punctate sculpture extends onto subsequent terga. Second metasomal tergum, anterior to the area of micropunctures, there is a region with coriaceous-alutaceous sculpture, primarily on the dorsal part and extending laterally to the beginning of pubescence. Ventral area of second metasomal tergum pubescent, obscuring sculpture in this region. The combination of coriaceous-alutaceous sculpture and pubescence restricts the smooth and shining area to a very limited region. Projecting part of hypopygial spine long (Fig. 14A); 7 × as long as high in lateral view; ventrally tapering in width towards apex, laterally with long setae that may exceed the width of ventral spine distally, not forming an apical patch.

Male: Differs from female as follows: 5 mm (n = 2; 4.7 mm / 5.2 mm). Head (Fig. 14D), in dorsal view, 2.15 × wider than long. POL 1.6 × the DOL. Transfacial line 1.4 × height of an eye. Clypeus shinier and less rugose. Antennae with 15 antennomeres (Fig. 14C); F1 slightly modified, flattened on ventral side; elongate placodeal sensillae visible on all flagellomeres. Antennae and legs longer relative to the body (Fig. 15B). Mesoscutellum more widely and deeply emarginated on posterior margin (Fig. 14E). Posterodorsal extension of the body of the subaxillular strip, shorter, not reaching half height of mesoscutellum. Metasoma smaller than thorax (contrary to females, Fig. 15B). Metasoma (Fig. 14G) with less ventral pubescence and less extensive coriaceous-alutaceous sculpture; smooth and shining sculpture covering one-third of second metasomal tergum. Metatibia 1.5 × as long as metatarsus. Metafemur more slender. Fore wings (Fig. 15D) more heavily infuscate across their entire surface; darker anterior band remains visible and follows the same pattern as in female (Fig. 15C). Vein R1 in the radial cell more evident and longer. Vein 2r less projected into radial cell.

Gall (Fig. 15E, F)**:** The morphology of galls of this species is relatively variable due to their geographical distribution and number of host species within their range. Galls follow the general pattern for the genus, being regularly spherical with a spongy inner consistency. When fresh, the surface is rarely completely smooth and usually has a moist texture. In some cases, galls may be almost entirely smooth on the surface and feature a nipple at apex, slightly rugose across the entire surface without visible protuberances, or with small pointed protuberances scattered randomly (including the nipple at the apex of gall). Occasionally, the nipple at the apex is large. Typically, smooth galls correspond to those in growth phase or nearing full maturity, while rugose galls usually correspond to those that have stopped growing and begin to acquire coloration and characteristics of dry galls. They are monothalamic. Normally, light green in color with irregular white (or lighter green) spots scattered across the surface of gall. In some cases, coloration of the spots is difficult to discern but still present. When dry, turn light brown, although some may acquire a reddish hue. Even when dry, white spots on the surface are generally still visible. Galls of this species become fragile to the touch when dry. Epidermis is thin and firmly attached to the internal spongy tissue. Internally, a dense layer of pith surrounds the larval chamber, with looser fibrous tissue between this layer and the epidermis. Average longitudinal diameter is 5.66 cm, and average transversal diameter is 5.27 cm (longitudinal diameter ranging from 38 to 86 mm and transversal diameter ranging from 37 to 80 mm; n = 71).

Distribution.

Amphibolips zapoteco was found in the Sierra de Juárez, in northern Oaxaca State, between 2051 and 2466 m a.s.l.

Biology.

Only the sexual generation is known. Galls are known to occur on three species of *Quercus*: *Q*. *scytophylla*, *Q*. *crassifolia*, and *Q*. *elliptica*. They have also been recorded on a recognized hybrid of *Quercus*: *Q*. x *dysophylla*. Additionally, many galls have been collected from species of *Quercus* in the section *Lobatae*, where it is not possible to determine exact host species. Galls were collected in March and April, and insects emerged in April and May. Smaller galls often fail to yield adult *Amphibolips* due to parasitoid attacks or presence of inquilines; thus, the average measurements of galls are influenced by these factors.

Remarks.

Amphibolips zapoteco belongs to the same lineage as *A*. *idiopteryx* and *A*. *darioi* within the Oaxacan lineage (sensu Castillejos-Lemus *et al*., 2025).

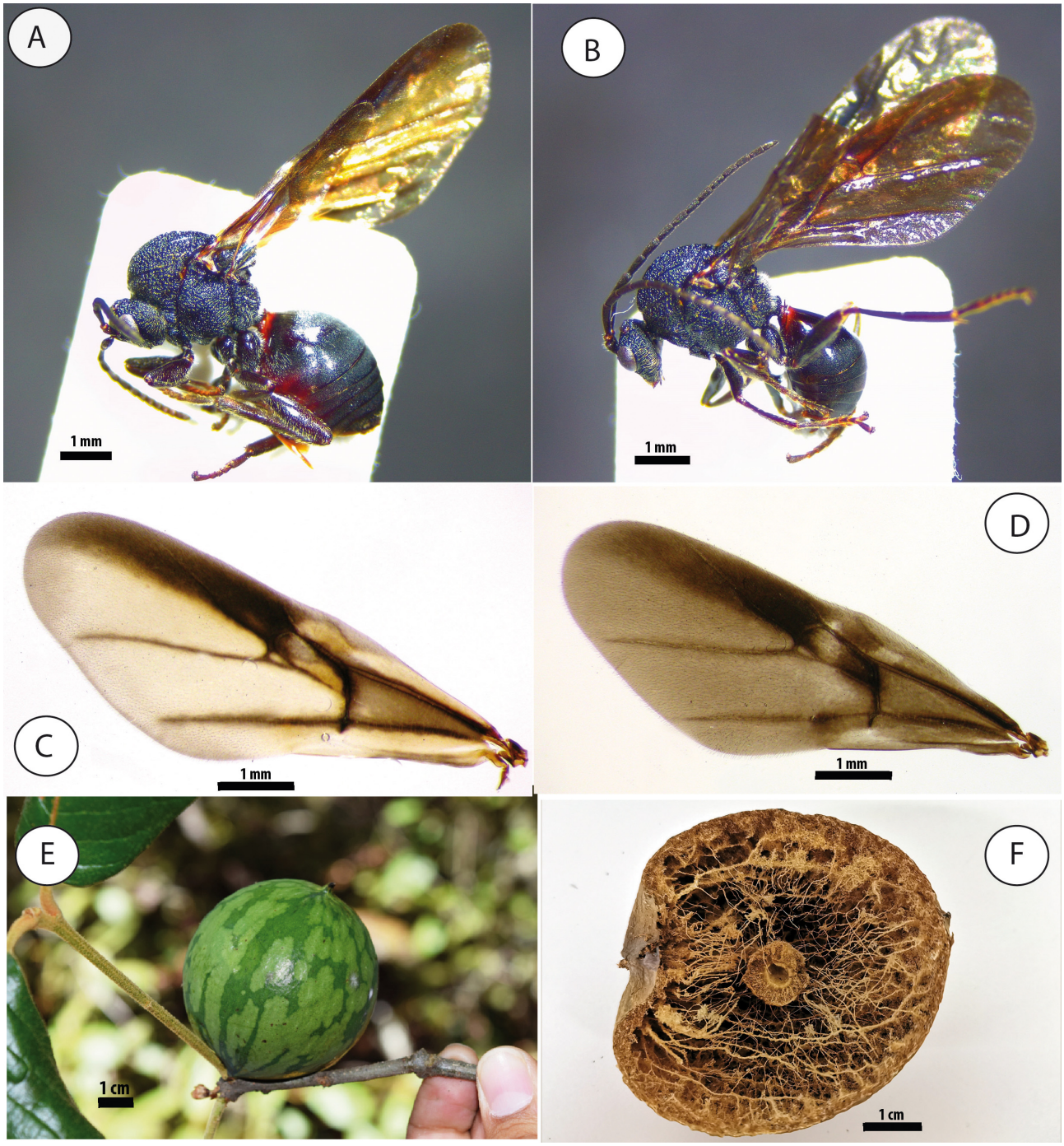

FIGURE 15. *Amphibolips zapoteco* sp. nov. **A** female habitus **B** male habitus **C** female fore wing **D** male fore wing **E** gall **F** section of a gall.

***Amphibolips darioi* Castillejos-Lemus & Nieves-Aldrey sp. nov.**
urn:lsid:zoobank.org:act:0142FEF7-6DCC-4763-A471-DA7415AAA661
Figs 16, 17

Type material.

Holotype.

MEXICO • female; Oaxaca state, San Miguel Suchixtepec; 16°06.968'N, 96°28.438'W; 2704 m a.s.l.; 24 Mar. 2017; D. Castillejos-Lemus leg.; ex gall on *Quercus* sp (*Quercus* sect. *Lobatae*), insect emerged on 3 Apr. 2017; mounted on a card in MNCN.

Paratypes.

MEXICO • 3m; same collection location; 16°06.013'N, 96°28.199'W; 2655 m a.s.l.; 24 Mar. 2017; D. Castillejos-Lemus leg.; ex gall on *Quercus crassifolia* (*Quercus* sect. *Lobatae*), insect emerged on 3 Apr. 2017; GenBank: SRX25798217 (individual code Amphibolips_sp_nov1_Oaxaca_341); 1m mounted on a card in MNCN, 1m mounted on a stub for SEM observation in ENES-Morelia, 1m preserved in alcohol at ENES-Morelia • 2m; same collection location; 16°04.282'N, 96°28.873'W; 2409 m a.s.l.; 24 Mar. 2017; D. Castillejos-Lemus leg.; ex gall on *Quercus crassifolia* (*Quercus* sect. *Lobatae*), insect emerged on 3 Apr. 2017; 1m mounted on a card in ENES-Morelia and 1m preserved in alcohol (extracted dead from the gall on 5 Dec. 2024).

Additional material (only galls).

MEXICO • 7 galls; same data as the paratype from 2655 m a.s.l.; 2 dissected and 5 complete; in ENES-Morelia and CNIN • 3 galls; same data as the paratype from 2409 m a.s.l.; 2 dissected and 1 complete; in ENES-Morelia and CNIN.

Etymology.

The specific epithet "*darioi*" is dedicated to Darío Alejandro, the son of the lead author, in gratitude for his support during this project.

Diagnosis.

Amphibolips darioi will be compared with other species from Oaxaca, following the same approach used for *A. idiopteryx* (see diagnosis of *A. idiopteryx*).

Amphibolips darioi differs from *A. idiopteryx*, as follows: vein R1 in radial cell, absent; pigmentation of the anal and basal cells, more evident in *A. idiopteryx*; unpigmented spot in the third cubital cell (Fig. 17B), clearly less extended than in *A. idiopteryx*; proportion of smooth and shining sculpture on second metasomal tergum, smaller (1/5); two longitudinal carinae on face, present (Fig. 16C); emargination on mesoscutellum, less pronounced. Additionally, their galls lack pointed protuberances or have only a few as the white spots on gall surface are barely perceptible (Fig. 17C). It differs from *A. zapoteco* as follows: vein R1 in radial cell, absent; clear spot in the third cubital cell, present; pigmentation of basal cell, more evident in *A. zapoteco*; two longitudinal carinae on face, present; emargination on mesoscutellum, less pronounced; a smooth depression below eyes, absent; pedicel is longer relative to the scape, as wide as long; malar space relative to the height of an eye, smaller; foveae are square and separated by a carina (Fig. 16B) and galls lack pointed protuberances or have only a few; white spots on gall surface, barely perceptible. It differs from *A. oaxacae* as follows: vein R1 in radial cell, absent; clear spot in the third cubital cell, present; pigmentation of the basal cell, more homogeneous in *A. oaxacae* (Fig. 18F); proportion of smooth and shining sculpture on the second metasomal tergum, smaller (1/5); two longitudinal carinae on face, present; emargination on mesoscutellum, less pronounced and white spots on gall surface, barely perceptible. It differs from *A. nigrialatus* as follows: *A. nigrialatus* has a generally darker pigmentation of fore wing; clear spot in *A. darioi*, present in the third cubital cell, whereas in *A. nigrialatus* this spot extends from the third cubital cell to discoidal cell (Fig. 18B); areolet present, absent in *A. nigrialatus*; vein R1 in radial cell, absent; malar space relative to the height of an eye, smaller; proportion of smooth and shining sculpture on the second metasomal tergum, smaller, 1/2 in *A. nigrialatus*; emargination on mesoscutellum, less pronounced.

Description.

Body length: 6 mm (n = 1) for females.

Female (Fig. 17A)**:** Body almost entirely black, most intensely so on the thorax, head, metasoma, and most of the antennae and legs. Distal part of the antennal scape and pedicel usually have a chestnut-colored region. The last flagellomeres chestnut ventrally and black dorsally. Mandibles chestnut. Mesosoma usually black, with tegulae and posterior region of propodeum immediately adjacent to the nucha chestnut. Tarsi typically brown. Metasoma usually black dorsally and chestnut ventrally. First metasomal tergum and anterior region of the second metasomal tergum adjacent to the first tergum, chestnut. Posterior margins of metasomal terga, beyond the bands of micropunctures, chestnut. Hypopygium and areas near hypopygium and ventral spine, chestnut, lighter on ventral spine. Fore wing (Fig. 17B) with a dark band extending along the anterior margin, covering the basal cell, first cubital cell, radial cell, costal cell, and anterior margin and junction with the radial cell in the third cubital cell. Entire discoidal cell, almost colorless, except in some cases where the edges of adjacent cells slightly invade its border, though this is barely noticeable. Costal cell has an unpigmented (or less intensely pigmented) area at the junction of vein Rs with vein R+Sc, which may in some cases extend towards the anterior margin of wing. Anal cell has little pigmentation but exhibits a more intensely pigmented spot along the posterior margin of wing, extending from the base of wing

and ending before vein M+Cu1; this also includes the distal edge of the cell. Veins R+Sc, Rs, and part of vein M that borders the basal cell are darkest, although in general, veins are visible due to some degree of color loss. Remaining veins are chestnut or light brown. Veins M (except in the basal cell) and Cu1 are light brown and typically the lightest compared to the other veins of the wing.

Head: in dorsal view, 2.5 × wider than long. POL 0.9 × OOL and 2 × DOL. Head, in anterior view (Fig. 16C), 1.3 × wider than high; gena slightly broadened behind the eye. Vertex, frons, lower face, and gena with strong reticulate-rugose sculpture. Face with two longitudinal carinae visible, extending from the ventral margin of toruli and converging towards the anterior tentorial pits; well-defined but diminishing as they approach the anterior tentorial pits. Irradiating carinae from clypeus, absent. Head moderately pubescent, less pubescent on vertex and frons. Clypeus more or less hexagonal, ventral margin strongly projecting over mandibles and sinuate on anterior margin. Anterior tentorial pits, well visible; epistomal sulcus and clypeo-pleurostomal lines, discernible. Above the epistomal sulcus, there is a protuberance that projects slightly over the clypeus (more evident in males; Fig. 16C). Malar space 0.6 × the height of the compound eye. Toruli situated at the mid-height of the compound eye. Transfacial line 1.6 × the height of an eye. Distance between antennal rim and compound eye equal to the width of the torulus including rim. Ocellar plate slightly raised.

Mouthparts: Mandibles, strong and exposed; with dense setae in base.

Antenna: of moderate length, with 13 antennomeres. Flagellum not broadening towards apex, covered with short, erect setae. Pedicel short and small, as broad as long (Fig. 16F).

Mesosoma: in lateral view (Fig. 16D), 1.15 × as long as high. Pronotum pubescent; lateral surface of pronotum with strong, irregular, reticulate-rugose sculpture. Pronotum medially short, though slightly larger than in other species; median pronotal length 0.3 × that of lateral pronotal length. Pronotal plate slightly distinct dorsally. Central region of the pronotum, smooth and shiny, quite conspicuous and broad compared to the rest of the pronotum, which exhibits rugosities and pubescence.

Mesonotum (Fig. 16A)**:** Mesoscutum pubescent, primarily in the anterior region, but setae are very short and thin, making them conspicuous only in anterior area near the pronotum. Sculpture, reticulate-rugose; interspaces, smooth and shining. Notauli not discernible. Longitudinal median impression barely perceptible, only noticeable next to the transscutal fissure. Anteroadmedian signa scarcely visible, extending backward to near one-third of mesoscutum, almost obscured by reticulate-rugose sculpture. Parapsidal signa well discernible but shallow, reaching the mid-length of mesoscutum or slightly shorter. Transscutal fissure narrow, almost straight. Mesoscutellum (Fig. 16B) as wide as long, approximately 0.45 × as long as mesoscutum. Strongly and coarsely rugose, slightly pubescent, with a median longitudinal impression that makes mesoscutellum emarginate posteriorly; median longitudinal impression extends anteriorly to the scutellar foveae. Scutellar foveae (Fig. 16B) 0.4 × as long as mesoscutellum, relatively square and deep, lacking pubescence, separated by a carina that arises in the posterior half and diminishes towards anterior region. Each fovea exhibits well-separated transverse rugae of variable length, with smooth interspaces. Axillula large, pubescent but with small setae, allowing the shiny background to be visible; dorsal part exhibits transverse rugae, while ventral part has a reticulate-rugose sculpture; posterior margin not delimited. In lateral view, the posterodorsal extension of the body of the subaxillular strip reaches 0.4 × the height of mesoscutellum. Mesopleuron reticulate-rugose, pubescent, with rugae not as strong as those on mesoscutum (Fig. 16D). Mesopleural triangle, shallow, slightly shinier than the rest of mesopleuron, particularly when compared to the adjacent area of mesopleuron, which is dull black. Presence of a posterior groove in the mesopleural triangle below tegula, this groove is deep and exhibits rugae with smooth interspaces, much more pronounced than in other known species.

Metanotum: Metapectal-propodeal complex. Metapleural sulcus reaching the posterior margin of mesopectus at approximately mid-height of metapectal-propodeal complex. Metascutellum rugose and broad. Metanotal trough pubescent, with the sculpture on the bottom smooth but not very shiny. Propodeal area with irregular rugae; pubescence present, primarily on sides. Lateral propodeal carinae, indistinct due to the rugae but weakly indicated due to reduced pubescence.

Legs: Densely pubescent, particularly on tibiae and tarsi; femora and tibiae robust. Metatibia 1.7 × as long as metatarsus; apical margin of metatarsomeres 1–4 with long, strong, erect setae. Metatarsal claws with strong, triangular basal lobes or teeth (Fig. 16E).

Fore wing (Fig. 17B)**:** slightly longer than body. Radial cell, approximately 4 × longer than wide; open along anterior margin, including the complete absence of vein R1. Areolet present, although vein M in this cell may appear diffuse due to loss of pigmentation. Veins M and Cu1 nearly straight, not reaching wing margin. Rs+M complete,

reaching basalis at mid-length, but slightly more than one-third of its length lacks pigmentation near its junction with vein M. First abscissa of radius (2r) curved, projected towards the radial cell, but projection is short. Vein Cu1, not branched into two veins, but exhibits a pigmented spot in the hypothetical region of vein Cu1b. Apical margin with very short or obsolete hair fringe. There is a small unpigmented spot at the end of the third cubital cell, very close to the anterior dark band; in some specimens, this spot is barely perceptible. Most densely pigmented regions are the costal cell, radial cell, and half of the basal cell adjacent to the costal cell.

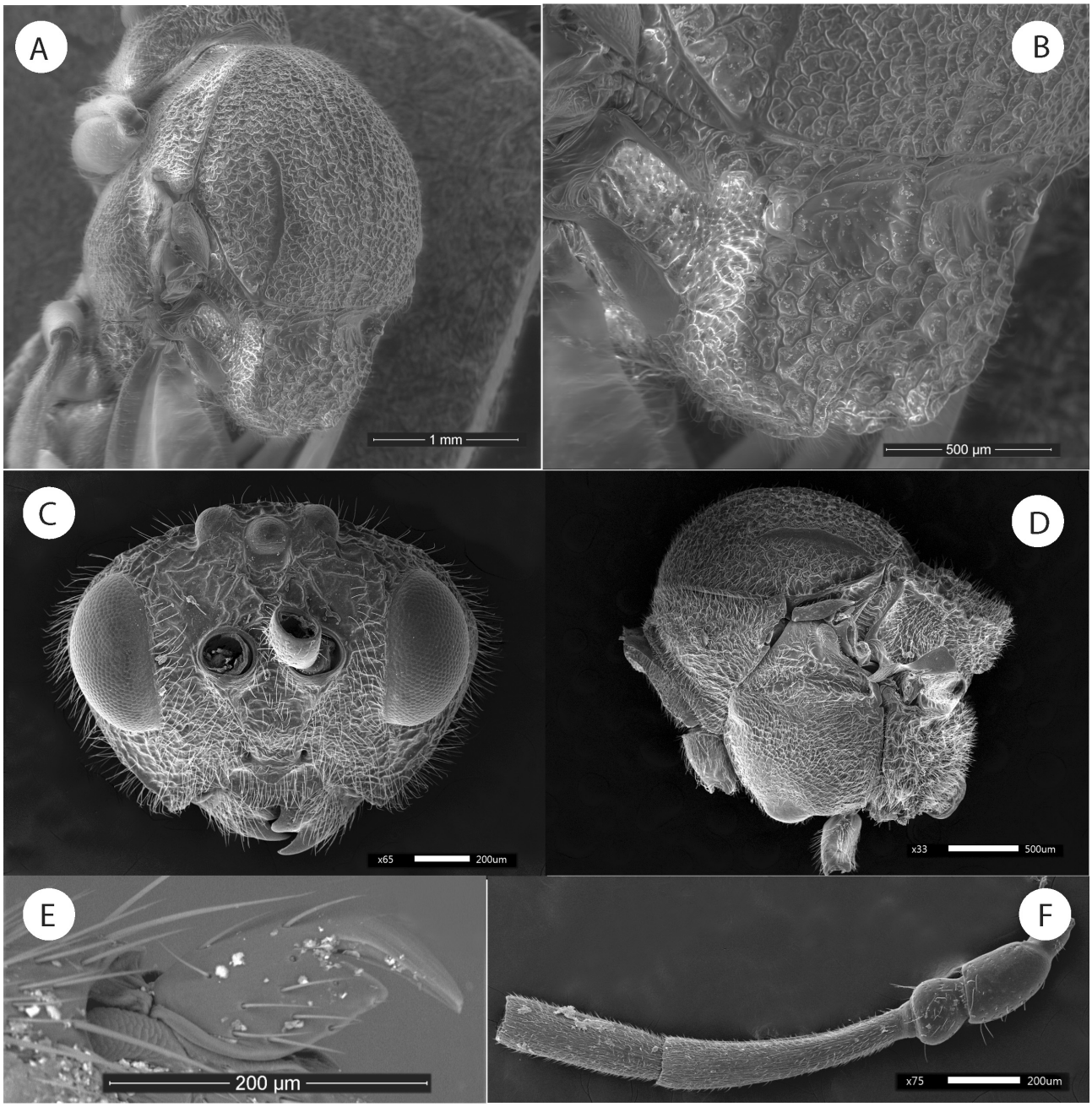

FIGURE 16. *Amphibolips darioi* sp. nov. **A** female mesosoma, dorsolateral view **B** female mesoscutellum **C** male head, anterior view **D** male mesosoma, lateral view **E** female metatarsal claw **F** male, detail of basal antennomeres.

Metasoma: in dorsal view, 1.5 × as long as wide; in lateral view, 1.3 × as long as high. Second metasomal tergum covering approximately 0.6 × the length of metasoma; anterior one-fifth shining, partially smooth; posterior third with a band of micropunctures clearly visible. In the second metasomal tergum, anterior to the area of micropunctures, there is a region comprising one-third of tergum with coriaceous-alutaceous sculpture, almost exclusively on dorsal part, following the anterior smooth area, but with a mixture of less dense micropunctures than

in posterior region, extending laterally. Punctate sculpture extends onto subsequent terga. Ventral area of second metasomal tergum pubescent, obscuring the sculpture in this region. Projecting part of hypopygial spine long, laterally with long setae, not forming an apical patch.

Male: Differs from female as follows: 5.7 mm (n = 1). Metasoma smaller than thorax (contrary to females). Antennae, legs, and wings longer relative to the body. Antennae with 15 antennomeres; F1 slightly modified (Fig. 16F), flattened on ventral side; elongate placodeal sensillae visible on all flagellomeres. Protuberance arising from the epistomal sulcus and projecting over the clypeus, more pronounced (Fig. 16C). Mesoscutellum, slightly more emarginated on posterior margin. Metasoma with sparse ventral pubescence and slightly visible coriaceous-alutaceous sculpture. Metatibia 1.4 × as long as metatarsus. Fore wings more heavily infuscate across their entire surface, but darker anterior band and unpigmented regions remain visible, following the same pattern as in female (Fig. 17B). Radial cell 3.6 × as long as wide.

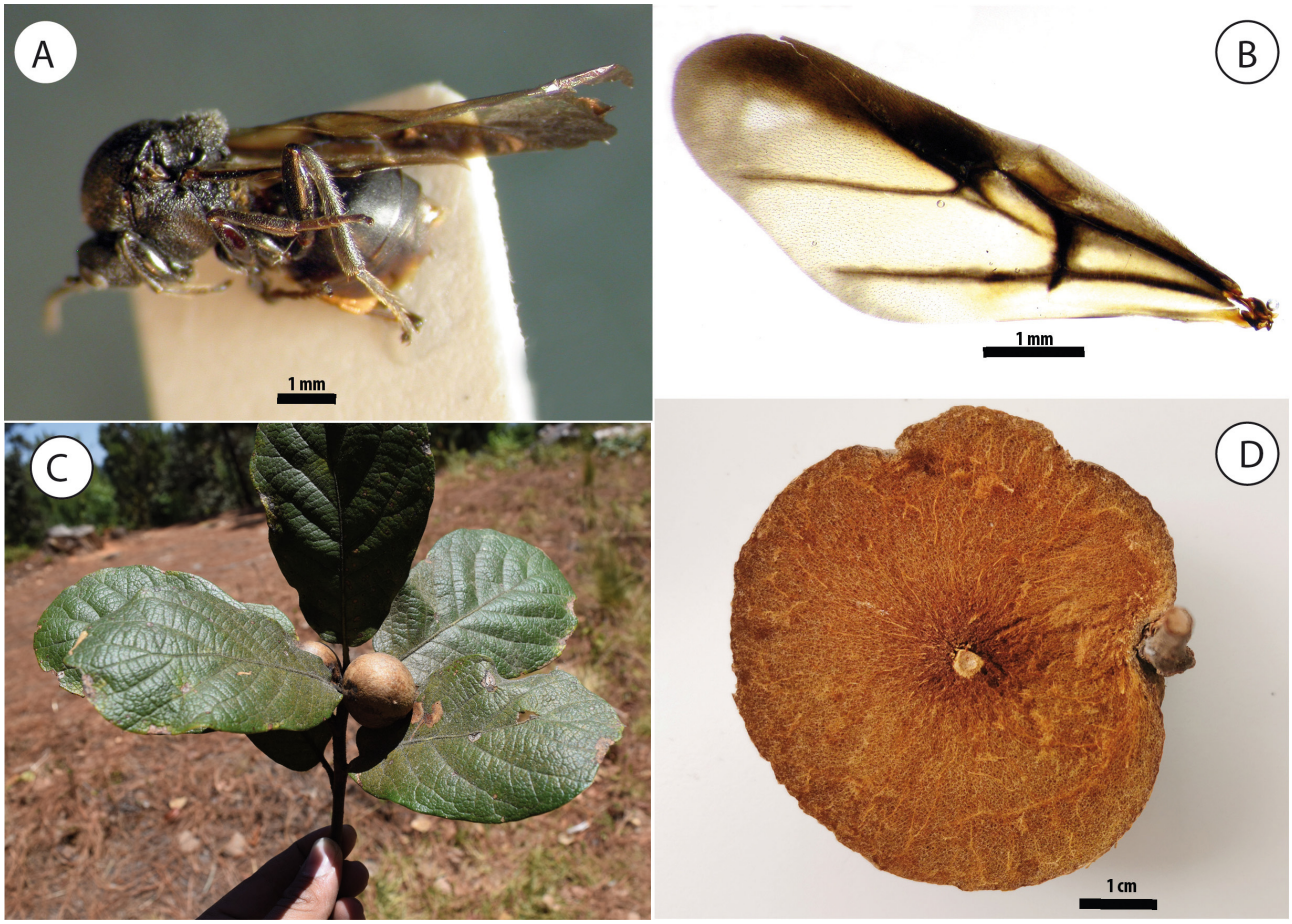

FIGURE 17. *Amphibolips darioi* sp. nov. **A** female habitus **B** female fore wing **C** gall **D** section of a gall.

Gall (Fig. 17C, D)**:** Gall is relatively spherical and exhibits typical characteristics of most *Amphibolips* species with similar galls. Surface, slightly rugose and smooth to the touch. They are monothalamic. When fresh, light green in color with small, faint white spots in areas that appear devoid of the green tone, which become difficult to discern when fully mature. As is typical for galls of this genus, galls of this species turn light brown when dry. The epidermis is thin and firmly attached to the internal spongy tissue when fresh. Internally, spongy tissue occupies the entire space between epidermis and larval chamber. When dry, galls become more fragile to the touch. Average longitudinal and transversal diameter is 6.6 cm (longitudinal diameter ranging from 42 to 73 mm and transversal diameter ranging from 46 to 79 mm; n = 10).

Distribution.

Amphibolips darioi was found in the municipality of San Miguel Suchixtepec, in the Sierra Sur region of Oaxaca state, at elevations between 2400 and 2700 m a.s.l.

Biology.

Only the sexual generation is known. Galls develop primarily on *Q*. *crassifolia*. They can be found at elevations between 2400 and 2700 m a.s.l. Galls were collected in March, and insects emerged in April.

Remarks.

Amphibolips darioi belongs to the same lineage as *A*. *idiopteryx* and *A*. *zapoteco* within the Oaxacan lineage (sensu Castillejos-Lemus *et al*. 2025).

Key to female *Amphibolips* species of clade IV (sensu Castillejos-Lemus *et al*. 2025)

Modified from Nieves-Aldrey *et al*. (2012) and Castillejos-Lemus *et al*. (2020) to include the newly described species. [Based on morphology, geographic distribution, and host-plant associations—as well as the lack of phylogenetic data—several additional species presumed to belong to clade IV (sensu Castillejos-Lemus *et al*. 2025) have also been incorporated.]

1. Fore wings either almost completely hyaline or only with a heavily infuscate spot on the basal area of radial cell (Fig. 18A); remainder of the fore wing, hyaline to only slightly infuscate. Metatarsal claws either simple or toothed. Metasomal tergites with or without conspicuous micropunctures. Mesoscutellum not or weakly emarginate posteriorly. Nearctic and Neotropical species, usually from USA with two species from Panama. . . . . *

* For this couplet run the species included in the clades I, II and III from the phylogenetic analysis of Castillejos-Lemus *et al*. (2025).

1'. Fore wings exhibiting any other pattern of pigmentation; almost entirely infuscate, infuscation never restricted to the radial cell, usually more heavily infuscate along the anterior margin of wing or exhibiting translucent transverse bands (Figs 5A, 12C, 18B–H). Metatarsal claws always with a strong acute basal lobe or tooth. Metasomal tergites strongly micropunctate. Mesoscutellum weak to strongly emarginate posteriorly. Predominantly Mexican species; at least one species from USA and other from Panama. Clade IV (Castillejos-Lemus *et al*. 2025). **2**

2. Fore wings with dark, heavily infuscated band along anterior margin (Figs 5C, 7C, 9B, 12C, 15C, 17B, 18E–H). This band may sometimes be interrupted but remains distinctly visible in the anterior wing region (Figs 9B, 18F, G). When hyaline spots are present, they typically occur in the distal wing area, usually restricted to the third cubital cell (Figs 12C, 17B) and rarely extending to the discoidal cell (Fig. 18B).. . . . . **3**

2'. Fore wings exhibiting translucent transverse bands crossing multiple cells in the distal region, without a clearly defined dark anterior transverse band (Fig. 18C, D). . . . . ..*

***** For this couplet option, first consult couplet six in the *Amphibolips* key by Cuesta-Porta *et al*. (2021), incorporating *A*. *palmeri* Bassett, 1890 and *A*. *trizonata* Ashmead, 1896 which are likewise absent from this key. Additionally, refer to couplets four and eleven in the *Amphibolips* key by Castillejos-Lemus *et al*. (2020), including *A*. *palmeri*, *A*. *trizonata*, *A*. *bassae* Cuesta-Porta & Pujade-Villar, 2020, *A*. *bromus* Pujade-Villar & Cuesta-Porta, 2020 and *A*. *turulli* Pujade-Villar & Cuesta-Porta, 2020 which are not covered in this key.

3. Notauli absent (Figs 10C, 13B, 16A). Extension of vein 2r into radial cell may be present. Distributed primarily south of TMVB (Trans-Mexican Volcanic Belt), occasionally east of TMVB (on the southern slopes) - in which case with hyaline spots in distal wing region (Fig. 18B).. . . . . ..**4**

3'. Notauli sometimes present (only in *A*. *nassa*, Fig. 19B). Extension of vein 2r into radial cell typically rare (only observable in *A*. *tarasco*). Never exhibiting hyaline spots in third cubital cell (nor discoidal cell), as they generally lack dark pigmentation beyond the anterior band or show uniform wing coloration (Figs 5C, 7C, 9B, 18E, G, H). Distributed primarily throughout TMVB, sometimes further north, particularly south of the Sierra Madre Occidental (SMOc). **8**

4. Areolet absent (Fig. 18B). Fore wings generally dark across most of their surface. Exhibits a hyaline band in the distal wing portion crossing from the third cubital cell to the discoidal cell (Fig. 18B). Face with two longitudinal carinae extending from the ventral margin of toruli and converging towards the anterior tentorial pits (Fig. 19A). Mesoscutellar foveae undivided by a carina. Vein 2r not projecting into the radial cell. Propodeal carinae visible. Coriaceous-alutaceous sculpture present on metasomal tergum II. Distributed east of TMVB (Trans-Mexican Volcanic Belt), on the southern slopes. . . . . ..***A. nigrialatus***

4'. Areolet present (Figs 12C, 15C, 17B, 18F). When hyaline spots occur, they are restricted to the third cubital cell (Figs 12C, 17B). Two longitudinal facial carinae may be present or absent. Mesoscutellar foveae may be divided by a carina or fused. Vein 2r may project into the radial cell. Propodeal carinae absent. Coriaceous-alutaceous sculpture present or absent on metasomal tergum II. Distributed south of TMVB, primarily in Oaxaca State. **5**

5. Hyaline spot in third cubital cell present (Figs 12C, 17B). Mesoscutellar foveae divided by a carina (Figs 10D, 16B). F1 1.6–1.7 × length of F2. Vein 2r projecting into radial cell. Coriaceous-alutaceous sculpture present on metasomal tergum II. **6**

5'. Hyaline spot in third cubital cell absent (Figs 15C, 18F). Mesoscutellar foveae either divided by a carina or fused (Fig. 13B). F1 1.3–1.6 × length of F2. Vein 2r may or may not project into radial cell. Coriaceous-alutaceous sculpture present or absent on metasomal tergum II.. . . . . ..**7**

6. Vein R1 in radial cell absent. Smooth and shining sculpture covering 1/5 of second metasomal tergum. Two longitudinal facial carinae present (Fig. 16C). Epistomal sulcus with slight protuberance projecting over clypeus (Fig. 16C). Mesoscutellar

emargination weakly pronounced (Fig. 16B). Galls either lacking pointed protuberances or with few protuberances (Fig. 17C). White spots on gall surface scarcely visible. Distributed in Sierra Sur, Oaxaca State. . . . . ***A. darioi* sp. nov.**

6'. Vein R1 in radial cell present but reduced. Smooth and shining sculpture covering 1/3 of second metasomal tergum. Two longitudinal facial carinae absent (Fig. 11A). Mesoscutellar groove more pronounced (Fig. 10D). Galls with distinct pointed protuberances (Fig. 12F). White spots on gall surface clearly evident. Distributed in Sierra Norte, Oaxaca State.. . . . . ***A. idiopteryx* sp. nov.**

7. Smooth and shining sculpture covering 1/5 of second metasomal tergum. Coriaceous-alutaceous sculpture present on metasomal tergum II. Smooth depression below eyes (Fig. 13A). Pedicel shorter relative to scape (0.25 ×), broader than long (Fig. 13C). F1 1.6 × length of F2. Malar space large relative to eye height (0.75 ×). Epistomal sulcus with slight protuberance projecting over clypeus (Fig. 13A). Mesoscutellar foveae ovoid, not divided by carina (Fig. 13B). Vein 2r slightly projecting into radial cell. Galls with pointed protuberances (Fig. 15E). Distributed in Sierra Norte, Oaxaca State. . . . . ***A. zapoteco* sp. nov.**

7'. Smooth and shining sculpture covering 3/4 of second metasomal tergum. Coriaceous-alutaceous sculpture absent on metasomal tergum II. No smooth depression below eyes. Pedicel longer relative to scape (0.5 ×). F1 1.3 × length of F2. Malar space small relative to eye height (0.5 ×). Mesoscutellar foveae elongated posteriorly, weakly divided by carina. Vein 2r not projecting into radial cell (Fig. 18F). Galls with smooth surface. Distributed in Istmo de Tehuantepec, Oaxaca State . . . . . ***A. oaxacae***

8. Costal cell strongly infuscated, at least in its proximal half where it meets the first cubital cell (Figs 5C, 7C, 18H). Notauli sometimes present (Fig. 19B). Propodeal carinae sometimes absent **9**

8'. Costal cell not infuscated or with very reduced pigmentation limited to the margin where it meets the first cubital cell (Figs 9B, 18E, G). Notauli absent (Fig. 8C). Propodeal carinae visible (Figs 8D, 19E) **10**

9. Mesoscutellar foveae fused and smooth (Fig. 19B). Notauli faintly visible posteriorly (Fig. 19B). Coriaceous-alutaceous sculpture absent on metasomal tergum II. Mesoscutellar emargination weakly defined (Fig. 19B). Propodeal carinae visible. Galls spherical with apical protrusions. On *Quercus castanea* in Michoacán State…..……***A. nassa***

9'. Mesoscutellar foveae either divided by a carina or fused with reticulate sculpture (Figs 2D, 4B). Notauli absent (Figs 2D, 6A). Coriaceous-alutaceous sculpture present or absent on metasomal tergum II. Mesoscutellar emargination distinct or weakly defined (Figs 2D, 6A). Anal cell with pigmented spot on posterior wing margin, apparently delimited anteriorly by vein 1A (Figs 5C, 7C). Propodeal carinae indistinct, obscured by irregular rugae. Galls spherical without apical protrusions (Figs 5F, 7B). On *Quercus scytophylla* and *Q. cualensis* in Jalisco State . . . . . ***A. megalokokka* sp. nov.**

•**Sexual generation (April–May):** Mesoscutellar foveae divided by a carina (Fig. 2D). Coriaceous-alutaceous sculpture present on metasomal tergum II. Mesoscutellar emargination distinct (Fig. 2D). Body length: 4.4–6.3 mm. Large galls, averaging 7.5 cm in diameter (Fig. 5F). On *Quercus scytophylla* in Jalisco State.

•**Asexual generation (November):** Mesoscutellar foveae fused with reticulate sculpture (Fig. 6A). Coriaceous-alutaceous sculpture absent from metasomal tergum II. Mesoscutellar emargination weakly defined (Fig. 6A). Body length: 4.6 mm. Galls of moderate size, averaging 4.5 cm in diameter (Fig. 7B). On *Quercus cualensis* in Jalisco State.

10. Lateral margin of compound eye shining, smooth, demarcated by a conspicuous carina visible in anterior view (Fig. 19C). Metasomal tergum II with small dorsal projection of punctures towards anterior margin (Fig. 19D). Fresh galls light green with pale spots on surface. Galls developing in autumn on *Quercus eduardi*, *Q. emoryi*, and *Q. viminea* in Zacatecas State . . . . . ***A. rulli***

10'. Lateral margin of compound eye rarely smooth, and when slightly smooth, never demarcated by a conspicuous carina. Metasomal tergum II lacking a band of micropunctures, or if present, never showing dorsal projection of punctures towards anterior margin. Fresh galls rarely exhibiting pale surface spots (Fig. 9C), but when present, occurring in spring galls. ..11

11. Mesoscutellar foveae not fused with the mesoscutellar emargination; distinct from remaining mesoscutellar sculpture (Fig. 8C). Coriaceous-alutaceous sculpture always present but reduced on metasomal tergum II. Basal cell and first cubital cell weakly infuscated (Fig. 9B). Galls with extremely fragile epidermis (Fig. 9D), occurring above 2,100 m elevation in central TMVB (Trans-Mexican Volcanic Belt). Michoacán State galls rugose, apically elongated and hanging tip-downwards due to weight (Fig. 9C–E). Mexico State galls irregular, lacking protuberances (see description) and non-apiculate . . . . . ***A. oyamai* sp. nov.**

11'. Mesoscutellar foveae typically indistinct from the mesoscutellar emargination, often fused to posterior mesoscutellar margin (except in *A. zacatecaensis*). Coriaceous-alutaceous sculpture variable on metasomal tergum II (when present, always more conspicuous; except in *A. chilito*). Basal cell consistently infuscated (though occasionally very faint in *A. hidalgoensis*, Fig. 18G). First cubital cell variably infuscated. Gall epidermis more rigid; shape apiculate, completely spherical, or fusiform with a strong carina . . . . . *

*For this couplet, consult couplet eleven in the *Amphibolips* key by Nieves-Aldrey *et al*. (2012), incorporating *A. chilito* (Cuesta-Porta *et al*. 2025), which is likewise absent from this key.

Discussion

The genus *Amphibolips* represents a monophyletic group currently comprising 67 species, including the five new species we described herein (Castillejos-Lemus *et al*. 2025). Clade IV was known to have a distribution predominantly south of the United States, with the exception of *A. trizonata* - a pattern that partially mirrors the distribution of

their host plants (*Erythromexicana* sensu Hipp *et al*. 2020). As previously noted in studies of *Amphibolips* (Melika *et al*. 2011; Nieves-Aldrey *et al*. 2012; Pujade-Villar *et al*. 2018; Castillejos-Lemus *et al*. 2020; Cuesta-Porta *et al*. 2020, 2021, 2023, 2025) and evidenced by phylogenetic relationships within the genus (Castillejos-Lemus *et al*. 2025), *Amphibolips* diversity remains far from being fully resolved. While the precise drivers of this high species diversity remain unclear, one possible explanation is the high rate of diversification of their host plants (Hipp *et al*. 2020) associated with the geologically complex topography of the region where these species inhabit (Ferrari *et al*. 2018).

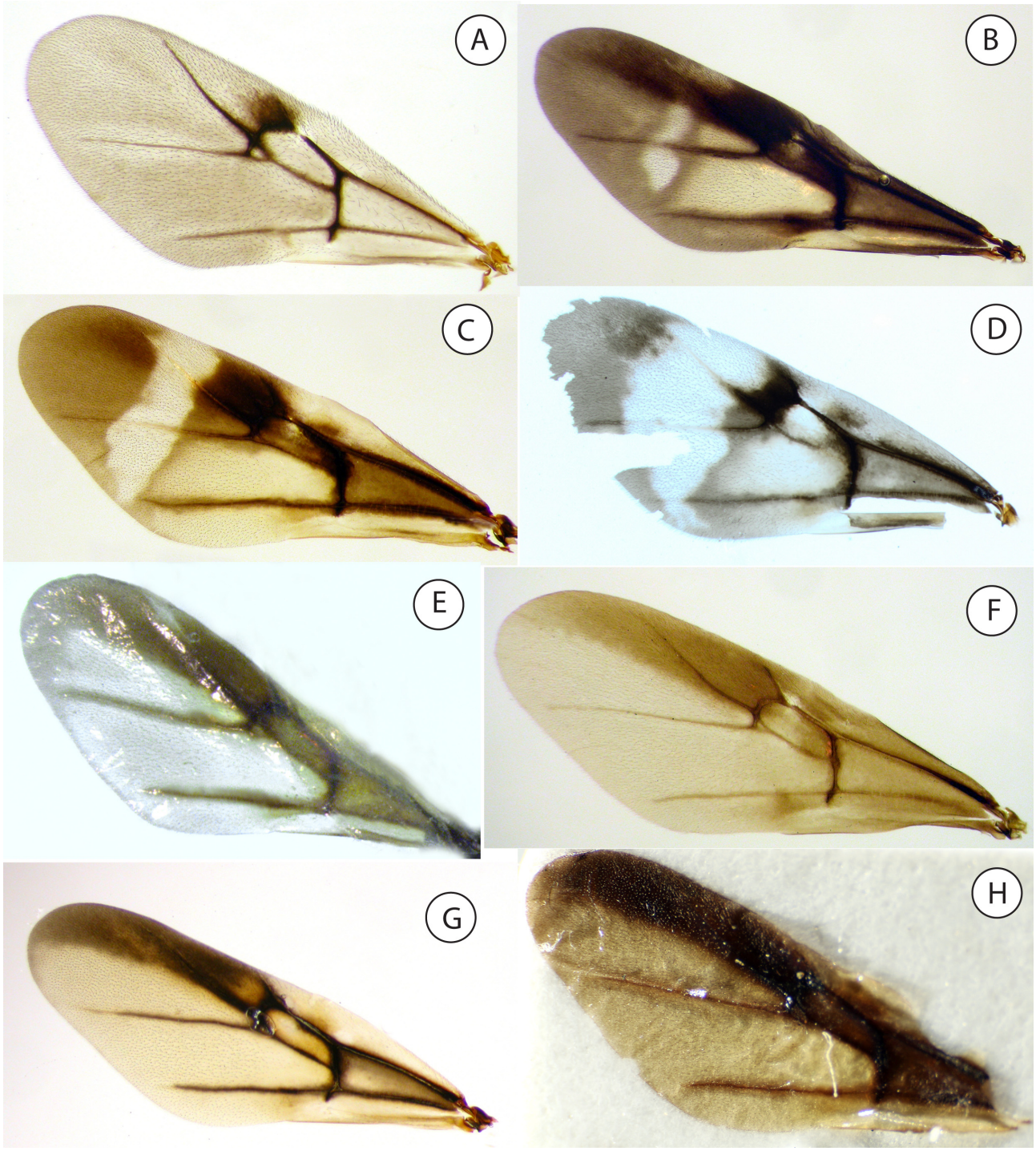

FIGURE 18. Fore wings of female *Amphibolips* species **A** *A. aliciae* Medianero & Nieves-Aldrey, 2010 **B** *A. nigrialatus* Nieves-Aldrey & Castillejos-Lemus, 2020 **C** *A. durangensis* Nieves-Aldrey & Maldonado, 2012 **D** *A. magnigalla* Nieves-Aldrey & Castillejos-Lemus, 2020 **E** *A. rulli* Pujade-Villar & Cuesta-Porta, 2020 (provided by Pujade-Villar and Cuesta-Porta) **F** *A. oaxacae* Nieves-Aldrey & Pascual, 2012 **G** *A. hidalgoensis* Pujade-Villar & Melika, 2011 **H** *A. nassa* Kinsey, 1937 (provided by Christine Le-Beau and Dr James Carpenter).

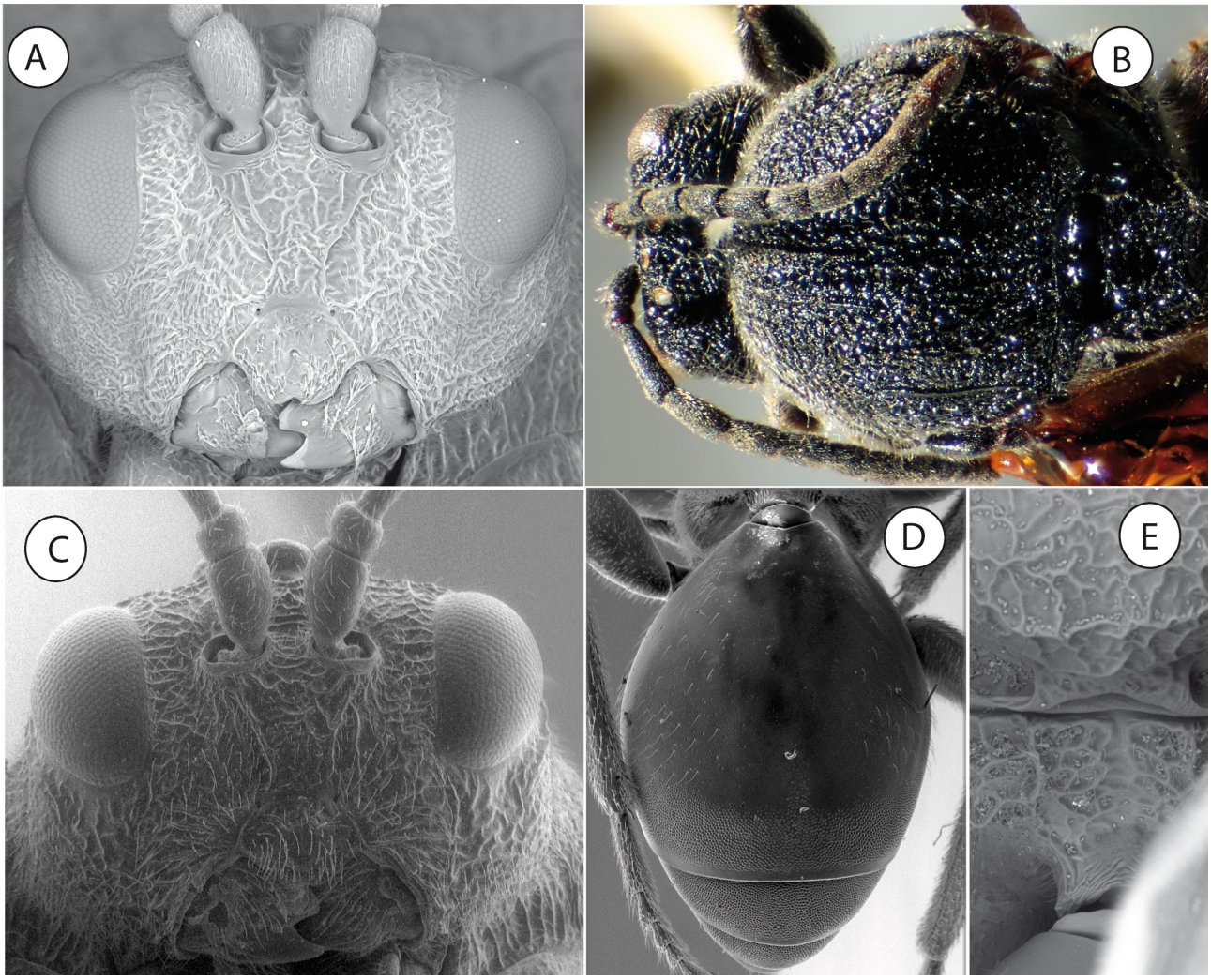

FIGURE 19. Diagnostic morphological characters of *Amphibolips* species **A** head of *A. nigrialatus* Nieves-Aldrey & Castillejos-Lemus, 2020, anterior view **B** mesosoma of *A. nassa* Kinsey, 1937, dorsal view (provided by Christine Le-Beau and Dr James Carpenter) **C** head of *A. rulli* Pujade-Villar & Cuesta-Porta, 2020, anterior view (provided by Pujade-Villar and Cuesta-Porta) **D** metasoma of *A. rulli*, dorsal view (provided by Pujade-Villar and Cuesta-Porta) **E** posterior border of mesoscutellum and propodeum of *A. zacatecaensis* Melika & Pujade-Villar, 2011, dorsal view.

Several hypotheses have been proposed regarding the morphology of galls of sexual and asexual generations of *Amphibolips* species (Nieves-Aldrey *et al*. 2012; Pujade-Villar *et al*. 2018). As noted by Castillejos-Lemus *et al*. (2025), galls in clade IV typically exhibit two distinct morphological types: semi-spherical galls with spongy parenchyma (*A. michoacaensis*) or spindle-shaped galls with firm-textured parenchyma (*A. fusus* Kinsey, 1937). Some galls display intermediate characteristics between these two types (e.g., *A. magnigalla*) although *A. magnigalla* from Oaxaca presents a sexual-generation with spindle-shaped galls. In other cases, *A. megalokokka* presents spherical gall morphology in both generations. *Amphibolips hidalgoensis*, one of the most frequently reported species in the literature (Cuesta-Porta *et al*. 2021), no males have been found despite having the typical spherical gall morphology for *Amphibolips* (Pujade-Villar *et al*. 2018; Cuesta-Porta *et al*. 2021). We are far from establishing patterns of gall morphology associated to sexual and asexual generations without comprehensive knowledge of the diversity of the genus. This difficulty may stem from attempting to identify patterns across distinct clades or lineages (Castillejos-Lemus *et al*. 2025). A potential solution would be to analyze species separately within each clade, enabling the development of alternative hypotheses to better understand species relationships within each lineage. Future studies integrating ecological and life-history data could further test hypotheses regarding the biology of closely related species within these subclades.

As mentioned in the diagnoses, certain *Amphibolips* species exhibit a dark, heavily infuscated band along the anterior region of the fore wing, while others display translucent transverse bands crossing several cells in the distal region of the wing, lacking a clearly defined dark anterior transverse band. This character state variation strongly supports our earlier suggestion that species from different clades should be treated separately. In Oaxaca, two distinct clades can be readily distinguished using this simple diagnostic character. However, it would be erroneous to group all species sharing either wing pattern as a single formal taxonomic unit - for instance, combining species from the SMOc clade (Castillejos-Lemus *et al*. 2025) with *A*. *magnigalla*, *A*. *kinseyi* Nieves-Aldrey & Castillejos-Lemus, 2020 and *A*. *dampfi* Kinsey, 1937. Nevertheless, this character proves useful for distinguishing species of the SMOc clade from those of the TMVB + South SMOc clade (Castillejos-Lemus *et al*. 2025). Some species remain challenging to assign to specific clades or lineages, such as *A*. *fusus* or *A*. *nigrialatus*, either due to their absence from phylogenetic studies or because of their complex relationships with other species. In the case of *A*. *fusus*, although it is recovered within clade IV, its position as sister to the SMOc + TMVB subclades rather than nested within them creates uncertainty about whether these subclades together form a single genus or multiple genera. For *A*. *nigrialatus*, the lack of molecular data means its placement within the Oaxaca subclade is inferred from morphology and biology, but cannot be tested. Both cases illustrate that formal generic recognition would require a more complete phylogenetic and taxonomic framework. A formal proposal to recognize these clades as distinct genera would require a comprehensive revision of the genus—including complete morphological diagnosability, expanded geographical sampling, and a stable phylogenetic hypothesis for all major lineages—efforts that remain to be undertaken.

Species differentiation within *Amphibolips* has proven challenging due to significant morphological similarity among taxa. However, this study provides novel insights into intraspecific morphological variation in both adult wasps and galls observed across slightly geographically separated populations. This pattern may reflect the rapid radiation of *Amphibolips* as a genus, potentially explaining the limited resolution along the backbone of the phylogenetic tree (Castillejos-Lemus *et al*. 2025). Furthermore, phylogenetic relationships based on molecular data appear sensitive to taxon sampling, potentially due to either unsampled extant lineages or extinct clades within certain regions.

We document substantial variability within *A*. *oyamai*, where specimens from Acuitzio and Sultepec exhibit morphological differences that might otherwise warrant species separation, yet available genetic evidence remains insufficient for such distinction (Castillejos-Lemus *et al*. 2025). For *A*. *oyamai*, expanded sampling across intermediate localities is needed to determine whether this represents exceptional intraspecific variation or undescribed sister species within the lineage. Similarly, the morphological variation between the two described generations of *A*. *megalokokka* illustrates how traditional taxonomy without molecular markers might erroneously classify them as distinct, albeit closely related species.

The size of the sexual-generation gall of *A*. *megalokokka* is notable, representing the largest known oak apple gall in the Americas and potentially worldwide. While a detailed analysis of the biological relevance of gall size is beyond the scope of this taxonomic work, this extreme morphology raises pertinent questions for future research. For instance, does gall size correlate with specific host oak species, environmental conditions, or confer a defensive advantage against parasitoids? Such extreme morphological traits highlight the potential for gall traits to serve as valuable characters in understanding species boundaries and adaptive evolution within *Amphibolips*, a genus already noted for its complex taxonomy.

Furthermore, Kinsey (1937) previously proposed hybridization among *Amphibolips* species in the *niger* complex, based on distribution patterns and host plant sympatry. Given the phylogenetic evidence (Castillejos-Lemus *et al*. 2025), observed species variability, and persistent taxonomic challenges, the potential role of hybridization in *Amphibolips* speciation warrants thorough investigation to clarify whether hybridization occurs and how it might impact species delineation.

We strongly recommend that future sampling efforts in biodiversity hotspots (like in the case of Mexico) should incorporate DNA analysis as a standard component of species descriptions, even in cases when only a single specimen is available. As demonstrated by Castillejos-Lemus *et al*. (2025), three legs from a single specimen often provide sufficient material for molecular marker extraction and amplification. The legs from one side of the specimen can be preserved while still allowing examination of potentially diagnostic morphological characters, although this is less critical for most *Amphibolips* species. Our recommendation stems from the recognition that intraspecific variation might be overlooked during species description. Molecular markers should be integrated

with morphological, phenological, host-plant, and geographic information to establish robust species boundaries. An equally important consideration is avoiding species assignments based solely on gall morphology (e.g. *A. michoacaensis*, *A. malinche* and *A. hidalgoensis*). Comprehensive evidence from multiple sources remains essential for accurate species determination.

Acknowledgements

This study forms part of the doctoral degree requirements for D.E.C.L. in the Programa de Posgrado en Ciencias Biológicas at the Universidad Nacional Autónoma de México (UNAM). Financial support was provided by the Secretaría de Ciencia, Humanidades, Tecnología e Innovación (SECIHTI) through a doctoral scholarship awarded to D.E.C.L. (Grant No. 330529). The authors express their gratitude to Javier Piña and Rafael Aguilar for field assistance, and to the local authorities of Sierra Juárez, Oaxaca, for facilitating fieldwork permissions. We acknowledge Laura Tormo and Alberto Jorge (Museo Nacional de Ciencias Naturales, MNCN), along with Orlando Hernández (Microscopy Laboratory, LAMIC, ENES Morelia, UNAM) for technical support with SEM imaging. Special thanks are extended to Christine Le-Beau (Scientific Assistant) and Dr. James Carpenter (Hymenoptera Curator) at the American Museum of Natural History (AMNH) for providing access to type specimens and sharing photographs of the *Amphibolips nassa* holotype from the collection. We are grateful to Dr. Miguel Ángel Alonso-Zarazaga for his expert guidance on the etymology of *Amphibolips megalokokka*. We extend our sincere gratitude to Charles Davis, Kristýna Bubeníková, an anonymous reviewer, Dr. Víctor Cuesta-Porta and Dr. Simon van Noort for their insightful comments, which significantly improved the manuscript.

References

Ashmead, W.H. (1896) Descriptions of new cynipidous galls and gall-wasps in the United States National Museum. *Proceedings of the United States National Museum*, 19 (1102), 113–136. https://doi.org/10.5479/si.00963801.19-1102.113

Barrera-Ruiz, U.M., Cibrián-Tovar, D., Llanderal-Cázares, C., González-Hernández, H., Rodríguez-Leyva, E. & Pujade-Villar, J. (2023) Biology of the sexual generation of *Loxaulus hyalinus* (Hymenoptera: Cynipidae) in *Quercus laeta* Liebm. oak groves in Mexico City. *Revista Chapingo serie ciencias forestales y del ambiente*, 29 (2), 147–163. https://doi.org/10.5154/r.rchscfa.2022.09.067

Bassett, H.F. (1890) New Species of North American Cynipidae. *Transactions of the American Entomological Society*, 17 (1), 59–92. [https://biostor.org/reference/127399]

Beutenmüller, W. (1909) The species of *Amphibolips* and their galls. *Bulletin of the American Museum of Natural History*, 26, 47–66.

Beutenmüller, W. (1911) Three new species of Cynipidae (Hym.). *Entomological News*, 22, 197–198. [https://www.biodiversitylibrary.org/page/2604288#page/249/mode/1up]

Beutenmüller, W. (1917) Descriptions of new Cynipidae. *The Canadian Entomologist*, 49 (10), 345–349. https://doi.org/10.4039/Ent49345-10

Burks, B.D. (1979) Superfamily Cynipoidea. *In*: Krombein, K.V., Hurd, P.D., Jr Smith, D.R. & Burks, B.D. (Eds.), *Catalog of Hymenoptera in America North of Mexico. Vol. 1. Symphyta and Apocrita*. Smithsonian Institution Press, Washington, D.C., pp. 1045–1107.

Castillejos-Lemus, D.E., Oyama, K. & Nieves-Aldrey, J.L. (2020) Description of three new species of oak gallwasps of the genus *Amphibolips* Reinhard from Mexico (Hymenoptera, Cynipidae). *ZooKeys*, 987, 81. https://doi.org/10.3897/zookeys.987.51366

Castillejos-Lemus, D.E., Nieves-Aldrey, J.L., Zhang, Y.M., Nicholls, J.A., Medianero, E., Rougon-Cardoso, A., Stone, G.N. & Oyama, K. (2025) Phylogenomic insights and geographic distribution of the New World genus *Amphibolips* Reinhard (Hymenoptera: Cynipidae, Cynipini) using ultraconserved elements. *Systematic Entomology*, 50 (2), 349–368. https://doi.org/10.1111/syen.12659

Cuesta-Porta, V., Barrera-Ruiz, U.M., Cibrián-Tovar, D. & Pujade-Villar, J. (2022) Discovery of the male of *Loxaulus hyalinus*, and implications for the sympatric species *Loxaulus laeta* (Hymenoptera: Cynipidae: Cynipini): an integrative taxonomical case of species delimitation. *Journal of Natural History*, 56 (5–8), 397–413. https://doi.org/10.1080/00222933.2022.2077150

Cuesta-Porta, V., Arnedo, M.A., Cibrián-Tovar, D., Barrera-Ruiz, U.M., García-Martiñón, R.D., Equihua-Martínez, A., Estrada-Venegas, E.G., Clark-Tapia, R., Romero-Rangel, S. & Pujade-Villar, J. (2020b) A new genus of oak gall wasp, *Striatoandricus* Pujade-Villar (Hymenoptera: Cynipidae: Cynipini) from America with descriptions of two new Mexican

species. *Zoological Studies*, 59, e8.
https://doi.org/10.6620/ZS.2020.59-08
Cuesta-Porta, V., Cooke-McEwen, C., Melika, G., Romero-Rangel, S., Equihua-Martínez, A., Estrada-Venegas, E.G., Clark-Tapia, R., Serrano-Muñoz, M., Chagoyán-García, C. & Pujade-Villar, J. (2024) Review of the Mexican species of *Disholcaspis* Dalla Torre & Kieffer with the description of eleven new species. *Zootaxa*, 5498 (1), 1–100.
https://doi.org/10.11646/zootaxa.5498.1.1
Cuesta-Porta, V., Equihua-Martínez, A., Estrada-Venegas, E.G., Cibrián-Tovar, D., Barrera-Ruíz, U.M., Ordaz-Silva, S., López-Sánchez, I.V., Melika, G. & Pujade-Villar, J. (2020) Revision of the *Amphibolips* species of the '*nassa*' complex from Mexico and central America (Hymenoptera: Cynipidae). *Zootaxa*, 4877 (1), 1–50.
https://doi.org/10.11646/zootaxa.4877.1.1
Cuesta-Porta, V., Equihua-Martínez, A., Estrada-Venegas, E.G., Romero-Rangel, S. & Pujade-Villar, J. (2025) A new species of *Amphibolips* (Hymenoptera: Cynipidae: Cynipini) from Mexico. *Zootaxa*, 5647 (5), 451–460.
https://doi.org/10.11646/zootaxa.5647.5.3
Cuesta-Porta, V., Melika, G., Equihua-Martínez, A., Estrada-Venegas, E.G., Cibrián-Tovar, D., Barrera-Ruíz, U.M., Ordaz-Silva, S., López-Sánchez, I.V. & Pujade-Villar, J. (2021) A new name for *Amphibolips kinseyi* Cuesta-Porta & Pujade-Villar and a revised key to the *Amphibolips* '*nassa*' species-complex from Mexico and Central America (Hymenoptera: Cynipidae). *Zootaxa*, 4938 (3), 331–345.
https://doi.org/10.11646/zootaxa.4938.3.4
Cuesta-Porta, V., Melika, G., Nicholls, J.A., Stone, G.N., Equihua-Martínez, A., Estrada-Venegas, E. & Pujade-Villar, J. (2023) Revision of the *Amphibolips* '*niger*' group with the description of a new species (Hymenoptera: Cynipini). *Zootaxa*, 5360 (4), 451–486.
https://doi.org/10.11646/zootaxa.5360.4.1
Ferrari, L., Orozco-Esquivel, T., Bryan, S.E., López-Martínez, M. & Silva-Fragoso, A. (2018) Cenozoic magmatism and extension in western Mexico: linking the Sierra Madre Occidental silicic large igneous province and the Comondú Group with the Gulf of California rift. *Earth-Science Reviews*, 183, 115–152.
https://doi.org/10.1016/j.earscirev.2017.04.006
García-Martiñón, R.D., Equihua-Martínez, A., Estrada-Venegas, E.G. & Pujade-Villar, J. (2024) A new Mexican species of *Andricus* that induces tuberous galls in *Quercus crassipes*. *Southwestern Entomologist*, 49 (4), 1389–1399.
https://doi.org/10.3958/059.049.0425
Guindon, S., Dufayard, J.F., Lefort, V., Anisimova, M., Hordijk, W. & Gascuel, O. (2010) New algorithms and methods to estimate maximum-likelihood phylogenies: assessing the performance of PhyML 3.0. *Systematic Biology*, 59 (3), 307–321.
https://doi.org/10.1093/sysbio/syq010
Harris, R. (1979) A glossary of surface sculpturing. *Occasional papers of the Bureau of Entomology of the California Department of Agriculture*, 28, 1–31.
Hartig, T. (1840) Ueber die Familie der Gallwespen. *Zeitschrift für die Entomologie*, 2 (3), 176–209. Available at: https://www.biodiversitylibrary.org/page/24565062
Hipp, A.L., Manos, P.S., Hahn, M., Avishai, M., Bodénes, C., Cavender-Bares, J., Crowl, A.A., Deng, M., Denk, T., Fitz-Gibbon, S., Gailing, O., González-Elizondo, M.S., González-Rodríguez, A., Grimm, G.W., Jiang, X.L., Kremer, A., Lesur, I., McVay, J.D., Plomion, C., Rodríguez-Correa, H., Schulze, E.D., Simeone, M.C., Sork, V.L. & Valencia-Avalos, S. (2020) Genomic landscape of the global oak phylogeny. *New Phytologist*, 226 (4), 1198–1212.
https://doi.org/10.1111/nph.16162
Hoang, D.T., Chernomor, O., von Haeseler, A., Minh, B.Q. & Vinh, L.S. (2018) UFBoot2: improving the ultrafast bootstrap approximation. *Molecular Biology and Evolution*, 35 (2), 518–522.
https://doi.org/10.1093/molbev/msx281
Kariñho-Betancourt, E., Hernández-Soto, P., Calderón-Cortés, N., Rendón-Anaya, M., Herrera-Estrella, A. & Oyama, K. (2020) Ecological genomics of plant-insect interactions: the case of wasp-induced galls. Evolutionary ecology of plant-herbivore interaction. *In*: Núñez-Farfán, J. & Valverde, P. (Eds.), *Evolutionary Ecology of Plant-Herbivore Interaction*. Springer Nature Switzerland AG, Cham, pp. 315–341.
https://doi.org/10.1007/978-3-030-46012-9_17
Kariñho-Betancourt, E., Hernández-Soto, P., Rendón-Anaya, M., Calderón-Cortés, N. & Oyama, K. (2019) Differential expression of genes associated with phenolic compounds in galls of *Quercus castanea* induced by *Amphibolips michoacaensis*. *Journal of plant interactions*, 14 (1), 177–186.
https://doi.org/10.1080/17429145.2019.1603404
Kinsey, A.C. (1937) New mexican gall wasps (Hymenoptera, Cynipidae). II. *Revista de Entomologia*, 7 (4), 428–471.
Liljeblad, J., Ronquist, F., Nieves-Aldrey, J.L., Fontal-Cazalla, F., Ros-Farré, P., Gaitros, D. & Pujade-Villar, J. (2008) A fully web-illustrated morphological phylogenetic study of relationships among oak gall wasps and their closest relatives (Hymenoptera: Cynipidae). *Zootaxa*, 1796 (1), 1–73.
https://doi.org/10.11646/zootaxa.1796.1.1
Liu, Z. & Ronquist, F. (2006) Familia Cynipidae. *In*: Fernández, F. & Sharkey, M.J. (Eds.), *Introducción a los Hymenoptera de la región Neotropical*. Sociedad Colombiana de Entomología y Universidad Nacional de Colombia, Bogotá, pp. 839–849.

Liu, Z., Engel, M.S. & Grimaldi, D.A. (2007) Phylogeny and geological history of the cynipoid wasps (Hymenoptera: Cynipoidea). *American Museum Novitates*, 2007 (3583), 1–48.
https://doi.org/10.1206/0003-0082(2007)3583[1:PAGHOT]2.0.CO;2

Martínez-Romero, A., Cuesta-Porta, V., Equihua-Martínez, A., Estrada-Venegas, E.D., Barrera-Ruiz, U.M., Cibrián-Tovar, D. & Pujade-Villar, J. (2022) Contribution to the knowledge of the Cynipini species (Hymenoptera: Cynipidae) in the Mexican states. *Revista mexicana de biodiversidad*, 93, e933998.
https://doi.org/10.22201/ib.20078706e.2022.93.3998

Medianero, E. & Nieves-Aldrey, J.L. (2010) The genus *Amphibolips* Reinhard (Hymenoptera: Cynipidae: Cynipini) in the Neotropics, with description of three new species from Panama. *Zootaxa*, 2360 (1), 47–62.
https://doi.org/10.11646/zootaxa.2360.1.3

Melika, G. & Abrahamson, W.G. (2002) Review of the world genera of oak cynipid wasps (Hymenoptera: Cynipidae, Cynipini). *In*: Melika, G. & Thuróczy, C. (Eds.), *Parasitic wasps: evolution, systematics, biodiversity and biological control*. Agroinform, Budapest, pp. 150–190.

Melika, G., Nicholls, J.A., Abrahamson, W.G., Buss, E.A. & Stone, G.N. (2021b) New species of Nearctic oak gall wasps (Hymenoptera: Cynipidae, Cynipini). *Zootaxa*, 5084 (1), 1–131.
https://doi.org/10.11646/zootaxa.5084.1.1

Melika, G., Pujade-Villar, J., Nicholls, J.A., Cuesta-Porta, V., Cooke-McEwen, C. & Stone, G.N. (2021a) Three new Nearctic genera of oak cynipid gall wasps (Hymenoptera: Cynipidae: Cynipini): *Burnettweldia* Pujade-Villar, Melika & Nicholls, *Nichollsiella* Melika, Pujade-Villar & Stone, *Disholandricus* Melika, Pujade-Villar & Nicholls; and re-establishment of the genus *Paracraspis* Weld. *Zootaxa*, 4993 (1), 1–81.
https://doi.org/10.11646/zootaxa.4993.1.1

Melika, G., Equihua-Martínez, A., Estrada-Venegas, E.G., Cibrián-Tovar, D., Cibrián-Llanderal, V.D. & Pujade-Villar, J. (2011) New *Amphibolips* gallwasp species from Mexico (Hymenoptera: Cynipidae). *Zootaxa*, 3105 (1), 47–59.
https://doi.org/10.11646/zootaxa.3105.1.2

Minh, B.Q., Schmidt, H.A., Chernomor, O., Schrempf, D., Woodhams, M.D., von Haeseler, A. & Lanfear, R. (2020) IQ-TREE2: new models and efficient methods for phylogenetic inference in the genomic era. *Molecular Biology and Evolution*, 37 (5), 1530–1534.
https://doi.org/10.1093/molbev/msaa015

Nicholls, J.A., Melika, G., Digweed, S.C. & Stone, G.N. (2022) Pairing of sexual and asexual generations of Nearctic oak gallwasps, with new synonyms and new species names (Hymenoptera: Cynipidae, Cynipini). *Zootaxa*, 5145 (1), 1–79.
https://doi.org/10.11646/zootaxa.5145.1.1

Nicholls, J.A., Stone, G.N. & Melika, G. (2018) A new genus of oak gallwasp, *Protobalandricus* Melika, Nicholls & Stone (Hymenoptera: Cynipidae: Cynipini) from California. *Zootaxa*, 4472 (1), 141–152.
https://doi.org/10.11646/zootaxa.4472.1.7

Nieves-Aldrey, J.L. (2001) *Hymenoptera: Cynipidae*. *In*: Ramos, M.A., Alba, J., Bellés, X., Gosálbez, J., Guerra, A., Macpherson, E., Martín, F., Serrano, J. & Templado, J. (Eds.), *Fauna Ibérica. Vol. 16*. Editorial CSIC-CSIC Press, Madrid, pp. 13–636.

Nieves-Aldrey, J.L., Nicholls, J.A., Tang, C.T., Melika, G., Stone, G.N., Pujade-Villar, J., Buffington, M., Maldonado, Y. & Medianero, E. (2021) Re-description and systematic re-appraisal of the genus *Kokkocynips* Pujade-Villar & Melika (Hymenoptera: Cynipidae: Cynipini), including new combinations of Nearctic species and the description of a new species from Panama. *Zootaxa*, 4938 (2), 205–232.
https://doi.org/10.11646/zootaxa.4938.2.3

Nieves-Aldrey, J.L., Pascual, E., Maldonado-López, Y., Medianero, E. & Oyama, K. (2012) Revision of the *Amphibolips* species of Mexico excluding the "*niger* complex" Kinsey (Hymenoptera: Cynipidae), with description of seven new species. *Zootaxa*, 3545 (1), 1–40.
https://doi.org/10.11646/zootaxa.3545.1.1

Pujade-Villar, J. & Ferrer-Suay, M. (2015) Adjudicació genèrica d'espècies mexicanes d'ubicació dubtosa descrites per Kinsey i comentaris sobre la fauna mexicana (Hymenoptera: Cynipidae: Cynipini). *Butlletí de la Institució Catalana d'Història Natural*, 79, 7–14. [https://revistes.iec.cat/index.php/BICHN/article/view/90469.001/139573]

Pujade-Villar, J., Barrera-Ruíz, U.M. & Cuesta-Porta, V. (2018) Description of *Amphibolips cibriani* Pujade-Villar n. sp. from Mexico (Hymenoptera: Cynipidae: Cynipini). *Dugesiana*, 25 (2), 151–158.
https://doi.org/10.32870/dugesiana.v25i2.7051

R Core Team (2025) R: A language and environment for statistical computing. R Foundation for Statistical Computing, Vienna. Available from: https://www.R-project.org/ (accessed 23 February 2026)

Reinhard, H. (1865) Die hypothesen über die fortpflanzungsweise bei den eingeschlechtigen gallwespen. *Berliner Entomologische Zeitschrift*, 9 (1), 1–13. [https://www.biodiversitylibrary.org/page/8541525]

Richards, O.W. & Davies, R.G. (1977) Hymenoptera. *In*: Richards, O.W. & Davies, R.G. (Eds.), *Imms' General Textbook of Entomology*. Springer, Dordrecht, pp. 1175–1279.
https://doi.org/10.1007/978-94-017-0472-4_30

Ronquist, F. & Nordlander, G. (1989) Skeletal morphology of an archaic cynipoid, *Ibalia rufipes* (Hymenoptera: Ibaliidae). *Entomologica Scandinavica Supplement*, 33, 1–60.

Sottile, S., Cerasa, G., Massa, B. & Lo Verde, G. (2022) *Andricus cydoniae* Giraud, 1859 junior synonym of *Cynips conifica*

Hartig, 1843, as experimentally demonstrated (Hymenoptera: Cynipidae: Cynipini). *Insects*, 13 (2), 200. https://doi.org/10.3390/insects13020200
Stone, G.N., Schönrogge, K., Atkinson, R.J., Bellido, D. & Pujade-Villar, J. (2002) The population biology of oak gall wasps (Hymenoptera: Cynipidae). *Annual Review of Entomology*, 47 (1), 633–668. https://doi.org/10.1146/annurev.ento.47.091201.145247
Valencia-A, S. (2004) Diversity of the genus *Quercus* (Fagaceae) in Mexico. *Botanical Sciences*, 75, 33–53. https://doi.org/10.17129/botsci.1692
Wang, L.G., Lam, T.T.Y., Xu, S., Dai, Z., Zhou, L., Feng, T., Guo, P., Dunn, C.W., Jones, B.R., Bradley, T., Zhu, H., Guan, Y., Jiang, Y. & Yu, G. (2020) treeio: an R package for phylogenetic tree input and output with richly annotated and associated data. *Molecular Biology and Evolution*, 37 (2), 599–603. https://doi.org/10.1093/molbev/msz240
Weld, L.H. (1964) *Supplement to Cynipoidea (Hym.) 1905–1950 (1952)*. Privately printed, Ann. Arbor, Michigan, 28 pp.
Yu, G., Smith, D.K., Zhu, H., Guan, Y. & Lam, T.T.Y. (2017) ggtree: an R package for visualization and annotation of phylogenetic trees with their covariates and other associated data. *Methods in Ecology and Evolution*, 8 (1), 28–36. https://doi.org/10.1111/2041-210X.12628
Zhang, Y.M., Egan, S.P., Driscoe, A.L. & Ott, J.R. (2021) One hundred and sixty years of taxonomic confusion resolved: *Belonocnema* (Hymenoptera: Cynipidae: Cynipini) gall wasps associated with live oaks in the USA. *Zoological Journal of the Linnean Society*, 193 (4), 1234–1255. https://doi.org/10.1093/zoolinnean/zlab001